



Variation of Photosynthetic Induction in Major Horticultural Crops Is Mostly Driven by Differences in Stomatal Traits

Ningyi Zhang^{1*}, Sarah R. Berman¹, Dominique Joubert², Silvere Vialet-Chabrand¹, Leo F. M. Marcelis¹ and Elias Kaiser^{1*}

¹ Horticulture and Product Physiology, Department of Plant Sciences, Wageningen University & Research, Wageningen, Netherlands, ² Biometris, Department of Mathematical and Statistical Methods, Wageningen University & Research, Wageningen, Netherlands

OPEN ACCESS

Edited by:

Carl-Otto Ottosen,
Aarhus University, Denmark

Reviewed by:

Hartmut Stützel,
Leibniz University Hannover, Germany
Ryo Matsuda,
The University of Tokyo, Japan

*Correspondence:

Ningyi Zhang
ningyi.zhang@wur.nl
Elias Kaiser
elias.kaiser@wur.nl

Specialty section:

This article was submitted to
Crop and Product Physiology,
a section of the journal
Frontiers in Plant Science

Received: 22 January 2022

Accepted: 14 March 2022

Published: 27 April 2022

Citation:

Zhang N, Berman SR, Joubert D,
Vialet-Chabrand S, Marcelis LFM and
Kaiser E (2022) Variation
of Photosynthetic Induction in Major
Horticultural Crops Is Mostly Driven
by Differences in Stomatal Traits.
Front. Plant Sci. 13:860229.
doi: 10.3389/fpls.2022.860229

Under natural conditions, irradiance frequently fluctuates, causing net photosynthesis rate (A) to respond slowly and reducing the yields. We quantified the genotypic variation of photosynthetic induction in 19 genotypes among the following six horticultural crops: basil, chrysanthemum, cucumber, lettuce, tomato, and rose. Kinetics of photosynthetic induction and the stomatal opening were measured by exposing shade-adapted leaves ($50 \mu\text{mol m}^{-2} \text{s}^{-1}$) to a high irradiance ($1000 \mu\text{mol m}^{-2} \text{s}^{-1}$) until A reached a steady state. Rubisco activation rate was estimated by the kinetics of carboxylation capacity, which was quantified using dynamic A vs. $[\text{CO}_2]$ curves. Generally, variations in photosynthetic induction kinetics were larger between crops and smaller between cultivars of the same crop. Time until reaching 20–90% of full A induction varied by 40–60% across genotypes, and this was driven by a variation in the stomatal opening rather than Rubisco activation kinetics. Stomatal conductance kinetics were partly determined by differences in the stomatal size and density; species with densely packed, smaller stomata (e.g., cucumber) tended to open their stomata faster, adapting stomatal conductance more rapidly and efficiently than species with larger but fewer stomata (e.g., chrysanthemum). We conclude that manipulating stomatal traits may speed up photosynthetic induction and growth of horticultural crops under natural irradiance fluctuations.

Keywords: induction, genotypic variation, light fluctuations, modeling, photosynthesis, Rubisco activation, stomatal opening

INTRODUCTION

Irradiance in canopies frequently fluctuates due to changes in solar angle, cloud movements, and wind-induced leaf movements (Percy, 1953; Kaiser et al., 2015). When irradiance increases, the rate of photosynthesis of a shade-adapted leaf does not immediately increase to a new steady-state level. Instead, leaf photosynthesis increases progressively, until it reaches a new steady-state level; this process is referred to as photosynthetic induction. The time needed for photosynthetic induction leads to a potential carbon loss, as during this time period, leaf photosynthesis operates

below its steady-state rate (Mott and Woodrow, 2000; Salter et al., 2019; Acevedo-Siaca et al., 2020). Thus, speeding up photosynthetic induction may increase the yields of crops grown under fluctuating light (Slattery et al., 2018; Tanaka et al., 2019; Acevedo-Siaca et al., 2020).

Photosynthetic induction is generally considered to be limited by three main processes: (1) photoactivation of enzymes involved in the regeneration and production of ribulose 1,5-bisphosphate (RuBP), (2) increase in the activation state of Rubisco, and (3) stomatal opening (Percy, 1953; Kaiser et al., 2015, 2018). Mesophyll conductance may also limit photosynthetic induction (especially when transitioning from darkness to light), but the importance of mesophyll conductance limitation for photosynthetic induction is currently under debate (De Souza et al., 2020; Liu et al., 2021; Sakoda et al., 2021). Large genotypic variation in photosynthetic induction rates has previously been found in many crop species (McAusland et al., 2016; Salter et al., 2019; Acevedo-Siaca et al., 2020; Yamori et al., 2020). For example, in rice, soybean, and cassava, the integrated net photosynthesis rate (A) during the first 5 min after a switch from low to high irradiance was affected by genotypic variation (Soleh et al., 2017; Acevedo-Siaca et al., 2020; De Souza et al., 2020). Quantifying the genotypic variations of photosynthetic induction and identifying the relevant physiological traits can help with trait selection for breeding high-yielding cultivars with optimized photosynthetic induction.

The activation of enzymes involved in RuBP regeneration is thought to be complete within the first 1–2 min of photosynthetic induction (Percy, 1953); the extent of this limitation was found to be relatively similar among closely related wheat genotypes (Salter et al., 2019). The extent to which Rubisco activation and stomatal opening limit photosynthetic induction vary more strongly among species, and these two limitations are often interlinked. For example, in rice, wheat, and soybean, photosynthetic induction was found to be limited by the rate of Rubisco activation and presumably driven by concentrations of Rubisco and Rubisco activase (Soleh et al., 2016; Salter et al., 2019; Acevedo-Siaca et al., 2020). However, some studies also showed a strong role of stomatal conductance (g_s) in the photosynthetic induction of rice and wheat (Adachi et al., 2019; McAusland et al., 2020; Qu et al., 2020; Yamori et al., 2020). In recent years, the activation of Rubisco during photosynthetic induction has been approximated by estimating the dynamics of maximum Rubisco carboxylation rate (V_{cmax}) during photosynthetic induction through dynamic A vs. intercellular CO_2 concentration (C_i) curves (Soleh et al., 2016; Taylor and Long, 2017; Salter et al., 2019). This requires a measure of photosynthetic induction at several C_i , allowing for the estimation of the time constants that describe several phases of V_{cmax} induction and the kinetics of changes in electron transport rate at high irradiance (Soleh et al., 2016; Taylor and Long, 2017; Salter et al., 2019).

In many species, such as cassava, tomato, *Arabidopsis*, and in some tropical trees and shrubs, photosynthetic induction tends to strongly correlate with stomatal traits (e.g., initial g_s in low irradiance or stomatal opening rate) (Valladares et al., 1997; Allen and Percy, 2000; Kaiser et al., 2016, 2020; De Souza et al., 2020). Increasing g_s has been found to speed up the

photosynthetic induction in rice and tomato (Kaiser et al., 2020; Sakoda et al., 2020; Yamori et al., 2020). Stomatal anatomy (e.g., stomatal density and size) affects g_s , including its kinetics. Smaller stomata tend to show lower initial g_s at low irradiance, but faster opening and closure kinetics (Drake et al., 2013; Giday et al., 2013; Kardiman and Ræbild, 2018; Zhang et al., 2019). However, this inverse stomatal size–speed relationship is not conserved across species, as guard cell shape (elliptical, dumbbell) and guard cell cytoskeleton, cell wall elasticity, number and activity of transporters, or ion channels, also affect the rapidity of the stomatal response (Elliott-Kingston et al., 2016; McAusland et al., 2016; Lawson and Vialet-Chabrand, 2019).

Studies investigating the photosynthetic induction have so far mostly been conducted on the major field crops (e.g., rice, wheat, and soybean) and species in forestry eco-systems (Valladares et al., 1997; Allen and Percy, 2000; McAusland et al., 2016; Salter et al., 2019; Acevedo-Siaca et al., 2020), which leave a knowledge gap for other economically important species, such as tomato, cucumber, lettuce, and chrysanthemum. Despite the fact that irradiance fluctuations mostly occur under open-field conditions, irradiance in greenhouses can also fluctuate substantially (**Supplementary Figure 1**; Marcelis et al., 2018). Irradiance fluctuations in greenhouses are caused by the movement of the sun and cloud, both of which affect the shade cast by the greenhouse structure, including shading screens and supplemental lighting and canopy self-shading. An important distinction between the open fields and greenhouses is a near-complete lack of wind in the latter, which presumably reduces the frequency of sunlight fluctuations, and increases their duration, in the greenhouse. Crop growth in greenhouses is often source-limited, i.e., limited by crop photosynthesis (Marcelis, 1994); hence, greenhouse crops that respond to irradiance fluctuations with high efficiency are likely to show increased growth rates. Despite this substantial relevance of dynamic photosynthesis for crop growth in greenhouses, studies on the genotypic variation of photosynthetic induction so far have not included the major greenhouse crops.

The objective of this study was to quantify the genotypic variation of photosynthetic induction in some of the world's major horticultural crops, such as tomato, cucumber, rose, chrysanthemum, lettuce, and basil. Furthermore, we aimed to elucidate the influence of the main factors that affect the rapidity of photosynthetic induction: Rubisco activation and stomatal opening, including the role of stomatal anatomy.

MATERIALS AND METHODS

Plant Material and Growth Conditions

The experiment was conducted from 28 January to 12 June 2020, in a compartment (8 × 8 m) of a Venlo-type glasshouse located in Wageningen, the Netherlands (52°N, 6°E). Four growth tables were situated in the compartment. All genotypes were grown in the same compartment to avoid artifacts caused by different growth conditions. In total, 19 genotypes of six horticultural crop species were used, including two flower crops, chrysanthemum (*Chrysanthemum morifolium*) and rose (*Rosa*

hybrida); two fruit vegetables, cucumber (*Cucumis sativus* L.) and tomato (*Solanum lycopersicum* L.); and two leafy vegetables, basil (*Ocimum basilicum*) and lettuce (*Lactuca sativa* L.; **Table 1**). Cultivars for each crop were chosen based on their commercially relevant traits as horticultural merchandise: cultivars of the flower crops differed in flower color and number, those of fruit vegetables differed in fruit size, and those of leafy vegetables differed in leaf color and texture. For basil, cucumber, lettuce, and tomato, seeds were sown in rockwool plugs (diameter: 2 cm). Following germination, the seedlings were transferred to rockwool cubes (10 × 10 cm). Chrysanthemum plants were grown in plastic pots (diameter: 14 cm) filled with potting soil. Rose plants were grown in rockwool cubes (7 × 7 cm).

For basil, cucumber, lettuce, and tomato, the seeds were sown weekly. For chrysanthemum and rose, the plants were cut back weekly at the third or fourth node, counting from the base, to allow for the formation of a new axillary bud. Two weeks after sowing seeds or cutting back plants, two plants per genotype were placed on a growth table in a grid of four rows (distance between rows: 50 cm; distance between plants within the row: 30 cm). Plant positions were randomized two times per week to minimize any effects of a heterogeneous climate in the greenhouse compartment on plant growth. Plants were placed on the growth table for 2–3 weeks (i.e., 4–5 weeks after sowing seeds or cutting back plants), after which the measurements were conducted. This protocol was repeated weekly until data of 7–9 replicates per genotype had been collected.

A mixture of high-pressure sodium lamps (600 W, Philips, Eindhoven, Netherlands) and white light-emitting diodes (LEDs) (GreenPower LED toplighting module, Signify, Eindhoven, Netherlands) were used between 02:00 and 18:00 (a photoperiod of 16 h). Lamps were switched on during the photoperiod whenever global radiation (GR) outside the greenhouse dropped below 150 W m⁻² and were switched off

when GR > 250 W m⁻². Photosynthetically active radiation (PAR) from both lamp types combined was, on average, 226 ± 16 μmol m⁻² s⁻¹ at the canopy level (mean ± S.D.; **Supplementary Figure 2**). A shading screen (HARMONY 4215 O FR, Ludvig Svensson, Hellevoetsluis, Netherlands) was closed when GR > 600 W m⁻² and was opened when GR < 500 W m⁻². Day and night temperatures were set to 20 and 19°C, respectively. Relative humidity was set to 60%. Climate settings were designed to provide reasonably optimal growth conditions for all genotypes, in discussion with greenhouse cultivation experts at the Wageningen University. Average values of daily PAR (from both solar light and supplemental lamps), air temperature, relative humidity, and [CO₂] inside the greenhouse during the experiment were 241 ± 48 μmol m⁻² s⁻¹, 21.5 ± 1.4°C, 63 ± 6%, and 445 ± 11 ppm, respectively (mean ± SD; **Supplementary Figure 3**). Plants were irrigated four times per day between 7:00 and 19:00 with a customized nutrient solution suitable for all six greenhouse crops (pH: 6.3; EC: 2.2 mS cm⁻¹; **Supplementary Table 1**).

Gas Exchange Measurements

Net photosynthesis rate (*A*) and stomatal conductance to water vapor (*g_s*) were measured on the youngest fully expanded leaf, using a gas exchange system (LI-6800, Li-Cor Bioscience, Lincoln, NE, United States) equipped with a 6 cm² leaf chamber fluorometer. No correction for the leaf area was needed for any of the gas exchange measurements as the leaves always fully filled the leaf chamber. All measurements were performed at an air temperature of 23°C, relative humidity of 65%, and a flow rate of air through the system of 500 μmol s⁻¹. Irradiance was provided by a mixture of red (90%) and blue (10%) LEDs in the fluorometer. Before any gas exchange measurement, single plants were preconditioned to a low irradiance (ca. 50 μmol m⁻² s⁻¹) for 40–60 min in the greenhouse compartment, using a custom-built shading construction. The shading construction was covered by opaque plastic films and with LEDs installed at the top, which produced an irradiance at around 50 μmol m⁻² s⁻¹ with 90% red and 10% blue colors. Preadaptation under the shading construction for 40–60 min was applied to ensure that during subsequent gas exchange measurements, the leaves were sufficiently shade-adapted to produce comparable data.

Photosynthetic induction was measured under a range of [CO₂]: 50, 100, 250, 400, 600, 800, and 1,000 ppm. At 400 ppm of CO₂, the leaf was first exposed to a low irradiance of 50 μmol m⁻² s⁻¹ for 30 min in the gas exchange chamber, after which the irradiance was increased in a single step to a high level (1,000 μmol m⁻² s⁻¹) for an additional 30 min. A low irradiance rather than darkness was used for the initial light conditions, as in natural environments; shade-adapted leaves are often suddenly exposed to high light (due to cloud movements or wind), whereas the exposure of an entirely dark-adapted leaf to a high irradiance is unlikely in nature and greenhouses. Gas exchange data was logged every 2 s. If a steady-state *A* value was not reached after 30 min under high

TABLE 1 | Horticultural genotypes used in the experiment, with abbreviations used throughout the text in brackets, and starting plant materials.

Crop	Commercial cultivar name (abbreviation)	Starting material
Basil	Eleonora (BEL) ¹ ; Emily (BEM) ¹ ; Rosie (BR) ¹	Seeds
Chrysanthemum	Anastasia (CHA) ² ; Baltica (CHB) ² ; Radost (CHR) ² ; Yellow Zemblá (CHY) ²	Cuttings
Cucumber	Hipower (CUH) ³ ; Mewa (CUM) ⁴ ; Proloog (CUP) ⁴	Seeds
Lettuce	Cecilia (LO) ⁴ ; Gardia (LGA) ⁴ ; Gilmore (LGI) ⁴	Seeds
Rose	Apple Park (RAP) ⁵ ; Avalanche (RAV) ⁶ ; Red Naomi (RRN) ⁵	Cuttings
Tomato	Brioso (TB) ⁴ ; Merlice (TM) ⁷ ; Sweeterno (TS) ⁴	Seeds

¹ Provided by Enza Zaden, NL; ² provided by Delliflor, NL; ³ provided by Nunhems (Basf), NL; ⁴ provided by Rijk Zwaan, NL; ⁵ provided by Schreurs, NL; ⁶ provided by Dümme Orange, NL; ⁷ provided by Bayer Crop Science, NL.

irradiance, measurements continued until A reached a steady state. For other $[\text{CO}_2]$, the leaf was clamped into the cuvette at $50 \mu\text{mol m}^{-2} \text{s}^{-1}$ for 5 min, after which the irradiance was increased to $1,000 \mu\text{mol m}^{-2} \text{s}^{-1}$ for 15 min. All measurements ($[\text{CO}_2] \times \text{genotype}$) were randomized. Every week, a group of new plants (one per genotype) was chosen and measurements at different $[\text{CO}_2]$ were randomized among these plants during the day, to avoid potential diurnal effects being entangled with treatment effects. Once photosynthetic induction was measured on a given plant, the particular plant was not used for another measurement for at least 40 min, to avoid interference from previous conditions. All gas exchange measurements were done between 8:00 and 16:00 h.

Leaf Anatomical and Physiological Measurements

Samples to measure the stomatal size and density were taken on the same leaf used for gas exchange measurements. In addition, leaf light absorbance and chlorophyll and carotenoid contents were measured.

Stomatal Imprints

Stomatal imprints were taken after the final gas exchange measurement on a given plant had been completed. Imprints were taken using a silicone impression material (Zhermack, Badia Polesine, Italy), with two technical replicates on the abaxial side and two technical replicates on the adaxial side of each leaf. The silicon was allowed to fully dry on the leaf before it was removed gently. Clear nail polish was applied to the imprint and allowed to dry. The dry nail polish was viewed under a microscope (Leitz Aristoplan; Leica Microsystems, Wetzlar, Germany) and photographed at 25X and 40X magnification (Digital-Sight DS-Ri-1; Nikon, Tokyo, Japan). Images were analyzed with ImageJ, using the CellCounter and ObjectJ plugins (National Institute of Health, Bethesda, MD, United States).

Leaf Optical Properties

Leaf reflectance and transmittance were measured in the range of 400–700 nm for both adaxial and abaxial sides of the leaf. The measurement system consisted of two integrating spheres, each connected to a spectrometer and a custom-made light source (Hogewoning et al., 2010).

Leaf Chlorophyll and Carotenoid Contents

After the completion of gas exchange measurements, a leaf sample of 0.75 cm^2 was taken from each leaf and stored at -80°C . Samples were extracted with 1.5 ml of *N,N*-Dimethylformamide (DMF) at -20°C for approximately 2 weeks (Wellburn, 1994). The absorption of the DMF solution was measured at 480, 647, 664, and 750 nm for chlorophyll *a*, chlorophyll *b*, and carotenoid contents, using a SpectraMax iD3 Microplate Reader (software version 1.2.0.0, Molecular Devices, San Jose, CA, United States) or a Genesys 15 UV-Visible spectrophotometer (Thermo Fisher Scientific, Waltham, United States). Concentrations were calculated according to the study by Wellburn (1994).

Calculations

Rate of A Induction

The induction state of photosynthesis (IS) was calculated as follows:

$$IS(t) = \frac{A(t) - A_i}{A_f - A_i} \quad (1)$$

where $A(t)$ ($\mu\text{mol CO}_2 \text{ m}^{-2} \text{ s}^{-1}$) is CO_2 assimilation rate at time t and 400 ppm CO_2 ; A_i ($\mu\text{mol CO}_2 \text{ m}^{-2} \text{ s}^{-1}$) is initial A at low irradiance (average A measured in the last minute of low irradiance at 400 ppm CO_2); A_f ($\mu\text{mol CO}_2 \text{ m}^{-2} \text{ s}^{-1}$) is final steady-state A reached in high irradiance, at 400 ppm CO_2 . The times to reach 20% (T_{20}), 50% (T_{50}), and 90% (T_{90}) of full induction state were determined as the moments at which IS was the closest to these percentages, based on the IS time course generated from Eq. 1.

Rate of V_{cmax} and J Induction

Based on photosynthetic induction measurements at different $[\text{CO}_2]$, A/C_i curves were generated from the data obtained every 2 s under different $[\text{CO}_2]$. First, respiration rate (R_d) was estimated according to the study by Laisk (1977), i.e., R_d was identified as the intercept with the y -axis of the common intersection point of A vs. C_i at low and high irradiance, using the last data points measured under low and high irradiance at atmospheric $[\text{CO}_2]$ below 400 ppm. Then, the model of Farquhar et al. (1980) (the FvCB model) was fitted to each A/C_i curve to provide transient values of V_{cmax} and electron transport rate (J) during photosynthetic induction (**Supplementary Method 1**). The response of V_{cmax} induction during the first 15 min after exposure to high irradiance was fitted to an empirical model that represents a two-phase exponential function of time (Salter et al., 2019):

$$V_{\text{cmax}}(t) = V_{\text{mi}} + (V_{\text{mf}} - V_{\text{mi}}) \left\{ f \left[1 - \exp\left(-\frac{t}{\tau_{\text{fast}}}\right) \right] + (1-f) \left[1 - \exp(-t/\tau_{\text{slow}}) \right] \right\} \quad (2)$$

where $V_{\text{cmax}}(t)$ is V_{cmax} at time t ; V_{mi} is initial V_{cmax} after exposure to high irradiance; V_{mf} is final V_{cmax} after 15 min of high irradiance exposure; τ_{fast} and τ_{slow} are time constants for the fast and slow phase of V_{cmax} induction; f is a weighting factor (value: 0–1).

Transient Stomatal and Non-stomatal Limitations

Transient stomatal and non-stomatal limitations during photosynthetic induction were calculated based on an elimination approach. First, using the FvCB model, instantaneous A during photosynthetic induction was calculated every 2 s, with estimated V_{cmax} and J and measured g_s every 2 s (i.e., V_{mt} , J_t , and $g_{s,t}$) as input parameters. Calculated A was compared with the measured A during photosynthetic induction to ensure that model outputs accurately predicted the observed data before applying the elimination approach (**Supplementary Presentation 1**). In case of mismatches, values of V_{mt} and J_t were

optimized to improve model predictions. Photosynthesis rate as affected by transient stomatal limitation (A_s) was calculated by removing the transient limitations of Rubisco and electron transport rate changes, by using final V_{cmax} and J (V_{mf} and J_f) at high irradiance and instantaneous g_s ($g_{s,t}$) during induction (Eq. 3; Wang and Jarvis, 1993).

$$A_s = \min\{A_c(V_{mf}, g_{s,t}), A_j(J_f, g_{s,t})\} \quad (3)$$

In this case, any difference between A_s and A_f can be seen as caused by incomplete stomatal opening during induction. Stomatal limitation (L_s) was then calculated using Eq. 4:

$$L_s = \frac{A_f - A_s}{A_f - A_i} \cdot 100 \quad (4)$$

Photosynthesis rate as affected by transient non-stomatal limitation (A_{ns}) was calculated by using instantaneous V_{cmax} and J (V_{mt} and J_t) during induction and final g_s ($g_{s,f}$) reached at high irradiance (Eq. 5; Wang and Jarvis, 1993).

$$A_{ns} = \min\{A_c(V_{mt}, g_{s,f}), A_j(J_t, g_{s,f})\} \quad (5)$$

In this case, any difference between A_{ns} and A_f can be seen as caused by the incomplete induction of V_{cmax} and J . Nonstomatal limitation (L_{ns}) was then quantified using Eq. 6.

$$L_{ns} = \frac{A_f - A_{ns}}{A_f - A_i} \cdot 100 \quad (6)$$

Kinetics of g_s Responses

The response of g_s to a single step change in light intensity was quantified using a dynamic g_s model (Viale-Chabrand et al., 2013; McAusland et al., 2016). The model describes the temporal response of g_s , using a time constant (k , min), an initial time lag (λ , min), and a steady-state g_s ($g_{s,f}$, mol m⁻² s⁻¹) reached a given irradiance:

$$g_s = (g_{s,f} - g_{s,i}) e^{-e^{\frac{\lambda-t}{k}+1}} + g_{s,i} \quad (7)$$

where $g_{s,i}$ is the initial g_s value at low irradiance (average g_s measured in the last minute of low irradiance at 400 ppm CO₂). The time constant, k , describes the rapidity of the g_s response, independent of the amplitude of variation in g_s . The value, e is Euler's number (2.71828). Based on k and $g_{s,f}$, the maximum slope of the g_s response to a step-change in irradiance (Sl_{max} , $\mu\text{mol m}^{-2} \text{s}^{-2}$), which combines the rapidity and amplitude of the response, was calculated:

$$Sl_{max} = \frac{g_{s,f} - g_{s,i}}{k \cdot e} \quad (8)$$

Theoretical Maximum Stomatal Conductance

The maximum stomatal conductance to water vapor ($g_{s,max}$) when all stomates open to their maximum extent was calculated based on the studies by Franks and Farquhar (2001) and Franks and Beerling (2009):

$$g_{s,max} = \frac{d \cdot SD \cdot a_{max}}{v(l + \frac{\pi}{2} \sqrt{\frac{a_{max}}{\pi}})} \quad (9)$$

where d is the diffusivity of water vapor in the air ($24.9 \times 10^{-6} \text{ m}^2 \text{ s}^{-1}$); v is the molar volume of air ($24.4 \times 10^{-3} \text{ m}^3 \text{ mol}^{-1}$); SD is stomatal density; a_{max} is the maximum pore area and is approximated as $\pi(\rho/2)^2$, where ρ is stomatal pore length and l is stomatal pore depth (assumed to be equal to guard cell width). Both ρ and guard cell width were measured from stomatal imprints (Supplementary Table 2). Based on the stomatal density and length obtained from abaxial and adaxial leaf surfaces, $g_{s,max}$ per leaf surface was calculated. Then, $g_{s,max}$ for a specific genotype was calculated as the sum of $g_{s,max}$ for both leaf surfaces.

Kinetics of Stomatal Pore Area Increase

When substituting $g_{s,max}$ in Eq. 9 with g_s obtained from gas exchange measurements, a_{max} represents the average stomatal pore area a across the leaf surface. Thus, the stomatal pore area and its kinetics during the stomatal opening were quantified by solving a from Eq. 9 (refer to details in Supplementary Method 2):

$$a = \left(\frac{\frac{\sqrt{\pi}}{2} \cdot g_s \cdot v + \sqrt{\frac{\pi}{4} (g_s \cdot v)^2 + 4 * SD * g_s * v * l}}{2 \cdot SD \cdot d} \right)^2 \quad (10)$$

It is important to note that the relationship between a and g_s is not linear, which can result in differences in temporal kinetics between both traits.

Coefficient of Variation

To evaluate the variation of traits among genotypes, the coefficient of variation (CV, %) was calculated:

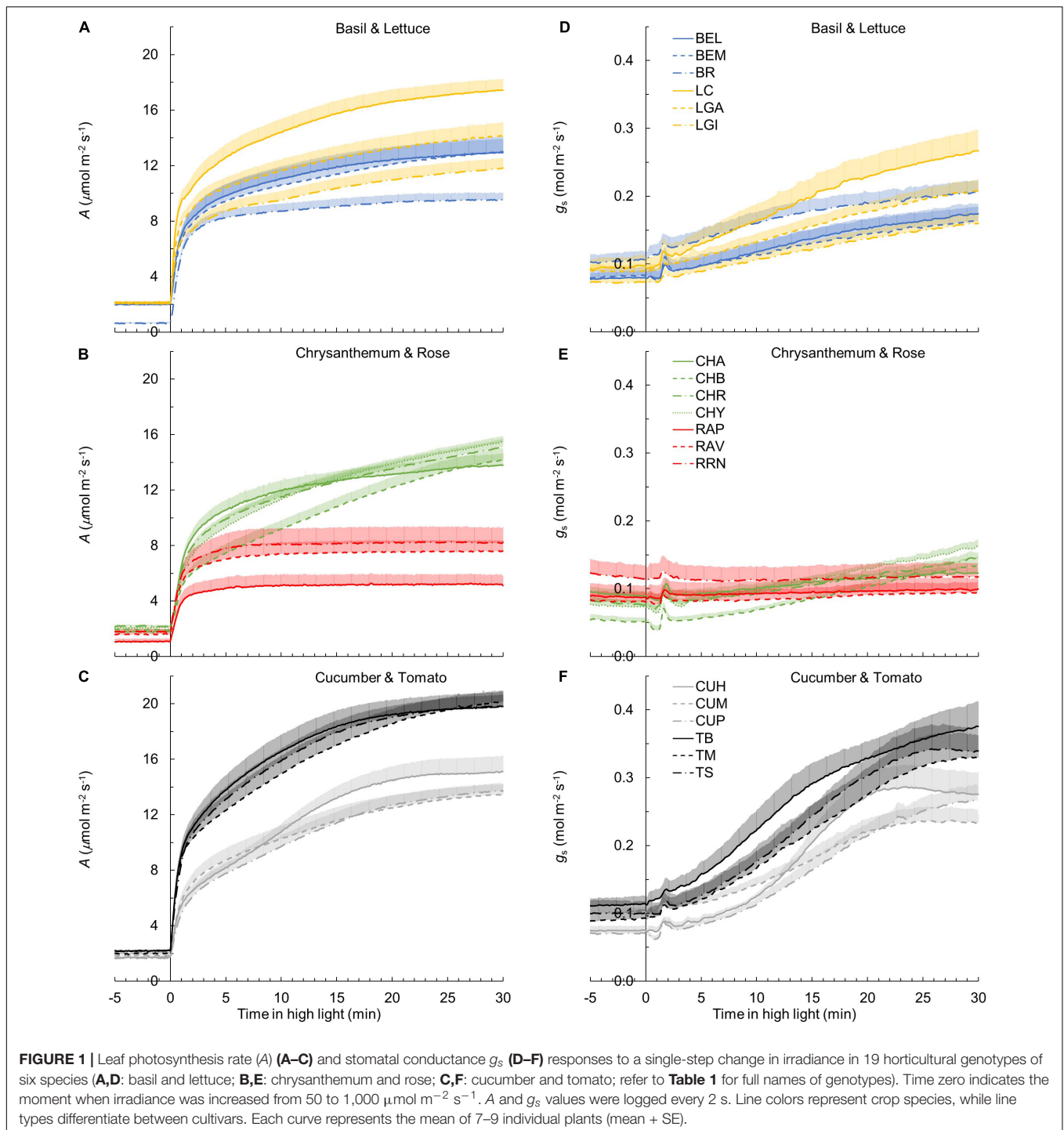
$$CV = \frac{X_{sd}}{X_{avg}} \cdot 100 \quad (11)$$

where X_{sd} and X_{avg} are, respectively, the standard deviation and mean value of the genotype-specific average of a given trait across all 19 genotypes.

Statistical Analysis

Using a nonlinear regression with the GAUSS method in PROC NLIN of SAS (SAS Institute Inc., Cary, NC, United States), parameters of the dynamic g_s model and V_{cmax} kinetics during A induction were estimated. Statistical analyses were conducted using R¹. First, normality was tested using the Shapiro-Wilk test, and homogeneity was tested using Levene's test to determine whether residuals showed equal variances. For traits that did not show equal variance, log transformation of data was applied. Differences between genotypes were detected using one-way ANOVA ($p < 0.05$), by taking into account, the different weeks of sowing/cutting as a block effect. When a significant difference was detected, a *post hoc* test was conducted for pairwise comparisons between genotypes, using Fisher's Protected Least Significant Difference (LSD) test ($p < 0.05$).

¹<http://www.r-project.org/>



RESULTS

Genotypic Variation of *A* and g_s Responses to a Single-Step Change in Irradiance

The kinetics of *A* induction varied substantially among the 19 horticultural genotypes tested (**Figures 1A–C**). Variation in

the key traits of photosynthesis dynamics tended to be larger between different crop species than between cultivars of the same species (**Figure 2**). CV of T_{20} , T_{50} , and T_{90} was 55, 61, and 42%, respectively, while CV of average *A* during the first 300 s of induction ($A_{\text{avg},300}$) was 22% (**Table 2**). The rate of *A* induction in rose was the fastest as demonstrated by small values for T_{50} and T_{90} in all three rose cultivars (**Figures 1B, 2A,B**).

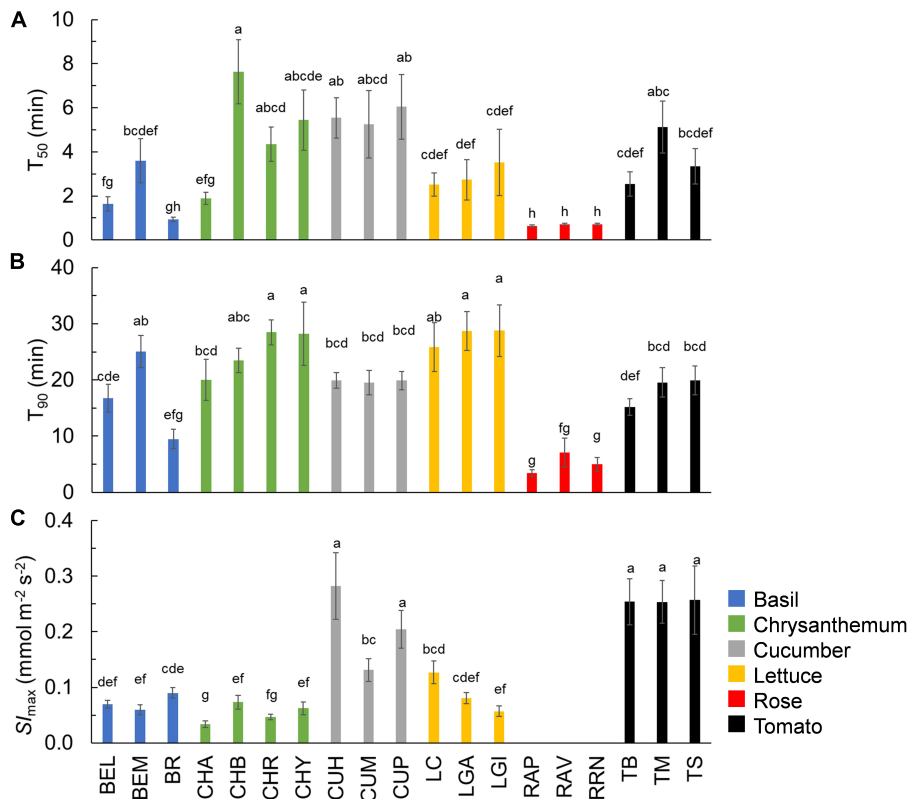


FIGURE 2 | Time needed for *A* to reach 50% (**A**: T_{50}) and 90% (**B**: T_{90}) of full photosynthetic induction, as well as the maximum rate of stomatal opening after an increase in irradiance (**C**: $S_{I_{max}}$) in 19 horticultural genotypes. Colors indicate crop species. Bars show means \pm SE ($n = 7-9$). Letters indicate significant differences ($p < 0.05$). For T_{50} , the result of the statistical test was based on log transformation of original data. $S_{I_{max}}$ was not estimated for rose. Refer to **Table 1** for full genotype names.

Chrysanthemum and lettuce, on the other hand, tended to have the highest T_{90} values (**Figure 2B**) and thus showed relatively slow induction. Chrysanthemum also had high T_{50} values, except for cv. Anastasia (CHA) had a very low T_{50} , whereas lettuce showed a relatively smaller T_{50} (**Figure 2A**). Tomato and cucumber had intermediate T_{50} and T_{90} (**Figures 2A,B**). Most crops showed a relatively small variation between cultivars, except for basil, which showed relatively large variations in T_{50} and T_{90} for its three cultivars (**Figures 2A,B**).

The kinetics of the g_s response to increases of irradiance also varied substantially among genotypes (**Figures 1D-F**). The value of g_s in rose barely responded to an irradiance increase; hence, $g_{s,i}$ and $g_{s,f}$ of rose cultivars were nearly identical (**Figure 1E** and **Supplementary Figure 4**). Therefore, the parameters representing the temporal response of g_s (k , λ , and $S_{I_{max}}$) were not estimated for rose. Values for the CV of k , $S_{I_{max}}$, and λ (among the remaining 16 genotypes) were, respectively, 23, 68, and 62% (**Table 2**). Both tomato and cucumber tended to have fast g_s increases, as well as exhibit stomatal oscillations (**Figure 1F**). Lettuce had medium $S_{I_{max}}$, followed by chrysanthemum and basil, which had a relatively smaller $S_{I_{max}}$ (**Figure 2C**). The CV of average g_s and water use efficiency in the first 5 min of *A* induction ($g_{s,avg,300}$ and $iWUE_{avg,300}$) were 22 and 21%, respectively, which were

smaller than CV for most dynamic g_s parameters (λ and $S_{I_{max}}$; **Table 2**).

Additionally, steady-state *A* and g_s varied strongly among genotypes (**Figures 1A-C**). A_i and $g_{s,i}$ had a CV of $\sim 20\%$ each (**Table 2**). For A_i , basil had the lowest value and tomato the highest, while for $g_{s,i}$, chrysanthemum showed the lowest value and rose showed the highest (**Table 2**). Steady-state *A* and g_s at high irradiance (A_f and g_f) showed CV of 30 and 46%, respectively, with tomato showing the highest and rose the lowest A_f and $g_{s,f}$ (**Table 2**).

Kinetics of Biochemical Parameters and Transient Limitations During Photosynthetic Induction

Based on dynamic *A* vs. C_i curves, the kinetics of V_{cmax} and J , as well as the stomatal and nonstomatal limitations to photosynthesis during *A* induction, were quantified (**Figure 3** and **Supplementary Figure 5**). Both V_{cmax} and J induction kinetics varied between crops and cultivars of the same crop (**Figures 3A,B** and **Supplementary Figures 5A,B**). After 15 min in high irradiance, V_{cmax} and J of rose were the smallest, while tomato and chrysanthemum showed higher values for final V_{cmax} and J (**Figures 3A,B**). Interestingly, tomato and lettuce showed

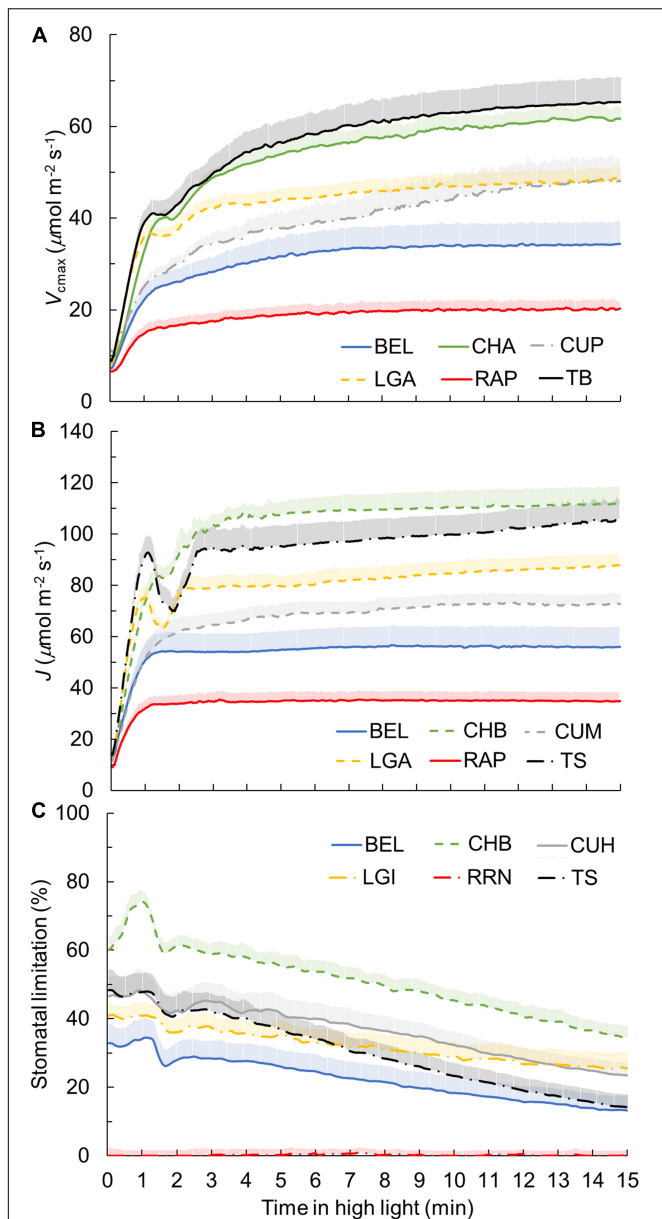


FIGURE 3 | Dynamics of maximum Rubisco carboxylation rate V_{cmax} (A), electron transport rate J (B), and stomatal limitations for photosynthesis (C) during photosynthetic induction for six representative genotypes. Each curve represents the mean of 6–7 individual plants (mean + SE). Genotypes showing the smallest and largest value for a given trait among all genotypes, as well as cultivars with an intermediate response for their crop, are shown. Refer to **Supplementary Figure 5** for representation of all 19 genotypes, as well as non-stomatal limitations for photosynthesis during photosynthetic induction.

transient drops in V_{cmax} and J induction during the first 3 min after exposure to high irradiance (**Figures 3A,B**). Variations in time constants for V_{cmax} induction were smaller than those describing A induction. Both τ_{fast} and τ_{slow} had CV values of 22% (**Table 2**). Generally, τ_{fast} varied between 0.5 and 1 min, with chrysanthemum showing the largest τ_{fast} (**Figure 4A**). The values of τ_{slow} of basil, chrysanthemum, cucumber, and

lettuce were generally around 5 min, and rose had the smallest τ_{slow} (3.1–3.6 min; **Figure 4B**). Surprisingly, large variations of τ_{slow} between cultivars were found in basil and tomato; basil cv. Eleonora (BEL) showed significantly smaller τ_{slow} than the other two basil cultivars, while tomato cv. Merlice (TM) showed a significantly larger τ_{slow} than the other two tomato cultivars (**Figure 4B**).

Within the first 15 min of exposure to high irradiance, transient non-stomatal and stomatal limitations of A induction showed substantial genotypic variation, with a greater variation in the level of transient stomatal limitation than in non-stomatal limitation (**Figure 3C** and **Supplementary Figures 5C,D**). Chrysanthemum showed the largest transient stomatal limitation among all crops, which went up to 70% during the first 1–2 min of induction and remained high (up to 40%) after 15 min in high irradiance (**Figure 3C**). Rose hardly exhibited any transient stomatal limitation during photosynthetic induction (**Figure 3C**), which can be explained by its non-responsive g_s to an irradiance increase (**Figure 1E**). Tomato showed a fast decrease in transient stomatal limitation (from ~50% to ~10% in 15 min) after an irradiance increase (**Figure 3C**). Transient non-stomatal limitation decreased sharply in the first 4–5 min after an irradiance increase (**Supplementary Figure 5C**). Most genotypes showed a transient non-stomatal limitation at around 10% after 15 min in high irradiance, except for cucumber, which still had ~20% nonstomatal limitation after 15 min of high irradiance (**Supplementary Figure 5C**). Some crops (basil, chrysanthemum, and tomato) also showed relatively large variations between cultivars for transient stomatal and nonstomatal limitations (**Supplementary Figures 5C,D**).

Genotypic Variation of Leaf Structural Traits

Stomatal density and size showed large CV, especially adaxially, and this was partly due to the fact that the rose had no stomata at the adaxial side (**Table 2**). The CV of stomatal density and size at the leaf abaxial side were, respectively, 78 and 57% (**Table 2**). Generally, large variation in the stomatal density and size occurred between crop species, while the variation between cultivars was relatively small (**Figures 5A,B**). Chrysanthemum had the largest, and cucumber had the smallest stomata (**Figure 5A**). Both chrysanthemum and lettuce had low stomatal density, while cucumber had the highest stomatal density (**Figure 5B**). These large variations in the stomatal density and size resulted in large variation in theoretical maximum stomatal conductance ($g_{s,max}$): the CV of $g_{s,max}$ was 50%, with cucumber showing the highest $g_{s,max}$ (up to ~5 mol m⁻² s⁻¹), followed by tomato (up to ~4 mol m⁻² s⁻¹), and lettuce, having the lowest $g_{s,max}$ (~1 mol m⁻² s⁻¹; **Figure 5C** and **Table 2**).

Using values of $g_{s,max}$ and observed g_s during photosynthetic induction (**Figures 1D–F**), absolute pore area opening was calculated. Kinetics of absolute pore area opening during A induction varied substantially between crops (**Figures 6A–C**). In cucumber leaves, individual pore area was found to be increased from ~1 to ~3 μm² after 30 min in high irradiance, resulting in

TABLE 2 | Definition, unit, maximum, minimum, mean, and coefficient of variation (CV) for dynamic, steady-state, anatomical and physiological traits across 19 horticultural genotypes.

Trait	Definition	Unit	Max. (genotype)	Min. (genotype)	Mean	CV (%)
Dynamic traits						
T_{20}	Time to reach 20% of full A induction	min	1.2 (CHB)	0.2 (RAP)	0.5	55
T_{50}	Time to reach 50% of full A induction	min	7.6 (CHB)	0.6 (RAP)	3.4	61
T_{90}	Time to reach 90% of full A induction	min	28.8 (LGI)	3.4 (RAP)	19.2	42
$A_{avg,300}$	Average A during the first 300 s of induction	$\mu\text{mol m}^{-2} \text{s}^{-1}$	10.9 (TB)	4.7 (RAP)	7.7	22
$g_{s,avg,300}$	Average g_s during the first 300 s of induction	$\text{mol m}^{-2} \text{s}^{-1}$	0.143 (TS)	0.052 (CHB)	0.099	22
$i\text{WUE}_{avg,300}$	Average intrinsic water-use efficiency during the first 300 s of induction ($A_{avg,300}/g_{s,avg,300}$)	$\mu\text{mol CO}_2 (\text{mol H}_2\text{O})^{-1}$	117 (CHB)	42 (RAP)	84	21
k	Time constant for g_s response to irradiance change ¹	min	16.2 (LGI)	7.6 (CUH)	10.8	23
Sl_{max}	Maximum rate of g_s response to irradiance change ¹	$\text{mmol m}^{-2} \text{s}^{-1}$	0.28 (CUH)	0.03 (CHA)	0.13	68
λ	Initial time lag of g_s response to irradiance change ¹	min	7.4 (CUP)	0.1 (BR)	3.9	62
f	Weighting factor (between 0–1) for the fast and slow phase of V_{cmax} induction	–	0.7 (LGA)	0.4 (CHY)	0.5	18
τ_{fast}	Time constant for fast phase of maximum Rubisco carboxylation rate (V_{cmax}) induction	min	1.1 (CHA)	0.5 (LC)	0.7	22
τ_{slow}	Time constant for slow phase of V_{cmax} induction	min	6.5 (TM)	3.1 (RAV)	4.8	22
Steady-state traits						
A_i	Steady-state A at low irradiance	$\mu\text{mol m}^{-2} \text{s}^{-1}$	2.2 (TS)	0.7 (BR)	1.9	21
A_f	Steady-state A at high irradiance	$\mu\text{mol m}^{-2} \text{s}^{-1}$	20.8 (TM)	5.7 (RAP)	14.4	30
ΔA	Difference between A_f and A_i	$\mu\text{mol m}^{-2} \text{s}^{-1}$	18.8 (TM)	4.5 (RAP)	12.5	33
V_{mi}	V_{cmax} at the start of photosynthetic induction	$\mu\text{mol m}^{-2} \text{s}^{-1}$	8.6 (CUP)	4.9 (BR)	7.0	16
V_{mf}	V_{cmax} 15 min after start of photosynthetic induction	$\mu\text{mol m}^{-2} \text{s}^{-1}$	65.9 (TB)	20.6 (RAP)	49.9	29
$g_{s,i}$	Steady-state g_s at low irradiance	$\text{mol m}^{-2} \text{s}^{-1}$	0.12 (RRN)	0.05 (CHB)	0.09	19
$g_{s,f}$	Steady-state g_s at high irradiance	$\text{mol m}^{-2} \text{s}^{-1}$	0.51 (TS)	0.10 (RAV)	0.25	46
Leaf anatomical traits and pigments						
SD_{ab}	Stomatal density at abaxial leaf side	mm^{-2}	340 (CUP)	40 (LGA)	124	78
SD_{ad}	Stomatal density at adaxial leaf side	mm^{-2}	267 (CUH)	0 (RAP, RAV, RRN) ²	67	133
SS_{ab}	Stomatal size at abaxial leaf side	μm^2	1411 (CHB)	210 (CUP)	681	57
SS_{ad}	Stomatal size at adaxial leaf side	μm^2	1325 (CHR)	0 (RAP, RAV, RRN) ²	540	81
$g_{s,max}$	Theoretical maximum g_s , if all stomates were to open to their maximum extent	$\text{mol m}^{-2} \text{s}^{-1}$	5.0 (CUP)	1.3 (LGI)	2.5	50
Leaf _{chl}	Leaf chlorophyll content ³	mg m^{-2}	222.0 (TM)	78.3 (LGA)	151.6	29
Chl <i>a</i> : <i>b</i>	Ratio of chlorophyll <i>a</i> to chlorophyll <i>b</i>	–	3.1 (LGA)	2.3 (BR)	2.7	7
Leaf _{caro}	Leaf carotenoid content	mg m^{-2}	28.4 (TM)	11.8 (BR)	19.1	25
Leaf _{abs}	Leaf light absorbance ⁴	–	0.89 (BR)	0.73 (LGA)	0.82	5

Maximum and minimum values are average values of 6–9 replicates.

¹Rose was excluded from estimations of k , Sl_{max} , and λ , due to a lack of change between $g_{s,i}$ and $g_{s,f}$.

²Rose did not display stomata on the adaxial leaf side.

³Sum of chlorophyll *a* and chlorophyll *b*.

⁴Average value of both leaf surfaces.

an increase of g_s from about 0.1 to 0.3 $\text{mol m}^{-2} \text{s}^{-1}$ (Figure 6C and Supplementary Figure 4). The pore area of tomato was calculated to increase more strongly, from ~ 4 to $\sim 16 \mu\text{m}^2$, leading to a g_s increase from about 0.1 to 0.4 $\text{mol m}^{-2} \text{s}^{-1}$ (Figure 6C and Supplementary Figure 4). In contrast, the pore area of chrysanthemum and lettuce required a larger extent of opening to achieve a comparable g_s increase with cucumber and tomato from ~ 18 to $\sim 36 \mu\text{m}^2$ in chrysanthemum and from $\sim 10 \mu\text{m}^2$ to $\sim 29 \mu\text{m}^2$ in lettuce (Figures 6A–C).

Surprisingly, when calculating the percentage of pore area opening relative to the maximum pore area, variation between crops was much smaller than for other traits (Figures 6D–F). During photosynthetic induction, all genotypes opened their stomata by less than 10% of the theoretical maximum pore area (calculated from pore length; Figures 6D–F). For example, the absolute pore area after 30 min in high irradiance reached $\sim 40 \mu\text{m}^2$ in chrysanthemum (which was the largest among all crops), which only accounted for 3–5% of the maximum pore

area (Figures 6B,E). The pore area of cucumber only reached $\sim 3 \mu\text{m}^2$ after 30 min in high irradiance, which was also $\sim 3\%$ of the maximum pore area (Figures 6C,F).

Leaf pigment concentrations showed relatively less variation among genotypes compared with most stomatal traits, with a CV of 25–30% for chlorophyll and carotenoid contents (Table 2). Since leaf color differed between cultivars (e.g., purple leaves in BR and brownish leaves in LGI), pigment types varied between crop species and cultivars (Supplementary Figures 6A,B). The chlorophyll *a:b* ratio showed little genotypic variation (CV: 7%), and an average of 2.7 across genotypes (Table 2). Leaf light absorptance was even more conserved, with a CV of 5%, the lowest value among all traits (Table 2). Small but significant differences in leaf light absorptance occurred between crop species, whereas variations between cultivars were not found, except for basil and lettuce which had cultivars (BR and LGI) with different leaf colors (Supplementary Figure 6C).

Trait Correlations

Generally, steady-state gas exchange traits correlated well with one another (e.g., $g_{s,f}$ vs. A_f , V_{mf} vs. A_f), as did dynamic traits (e.g., k vs. T_{90} ; Figure 7). Some steady-state traits also correlated well with dynamic traits (e.g., Sl_{\max} vs. $g_{s,f}$; Figure 7). Importantly, we identified key traits that showed strong correlations with indicators of the rate of photosynthetic induction (i.e., T_{20} , T_{50} , or T_{90}); these key traits were relevant to either stomata and their rate of movement ($g_{s,i}$ and k) or Rubisco activation (f , τ_{slow} , and V_{mf}) (Figure 8). Furthermore, these traits represented either dynamic (f , τ_{slow} , or k) or steady-state traits ($g_{s,i}$ or V_{mf}), suggesting that both types of the trait were relevant for the rate of photosynthetic induction. The value $g_{s,i}$ correlated negatively with T_{20} and T_{50} (Figures 8A,C). T_{20} was also correlated with f , and T_{50} was correlated with τ_{slow} (Figures 8B,D). Both k and V_{mf} were positively correlated with T_{90} , and k and T_{90} showed an especially strong linear correlation (Figures 8E,F). Given the strong correlations between photosynthetic induction traits (T_{20} , T_{50} , and T_{90}) and stomatal parameters ($g_{s,i}$ or k), we further tested whether stomatal conductance-related parameters were correlated with traits characterizing stomatal anatomy (stomatal size and density). The stomatal size was not correlated with either $g_{s,i}$, k , or Sl_{\max} , but was negatively correlated with stomatal density across species (except for chrysanthemum, which had large stomates; Supplementary Figures 7A–D). Interestingly, there was a very strong linear correlation between stomatal size on the abaxial side with that on the adaxial side of the leaf (Supplementary Figure 7E), with stomatal size on the adaxial leaf surface being $\sim 93\%$ of the size on the abaxial leaf surface for all species except for rose.

DISCUSSION

Large Variation in Induction Kinetics Exists in Major Horticultural Species

Increasing the rate of photosynthesis is expected to increase crop yields (Ort et al., 2015; Simkin et al., 2019). Although

the harvested product for horticultural crops can be very different from staple food crops, e.g., fresh flowers, fruits, and flavor additives, biomass production (thus photosynthesis) remains the basis for high yield and good product quality. For example, flower number was positively correlated with plant dry weight in chrysanthemum (Carvalho and Heuvelink, 2003), and extra assimilates contributed by the canopy improved the stem quality of cut-rose (Zhang et al., 2020). Therefore, increasing photosynthesis is important for optimizing horticultural crop production, especially where growth in most crops can be assumed to be a source rather than sink limited for most of the production season (Marcelis, 1994; Li et al., 2015).

Natural genetic variation is an important resource for breeding. The genotypic variation of photosynthesis has been examined widely regarding its steady-state traits (Flood et al., 2011). However, steady-state photosynthesis does not provide an accurate representation of operating photosynthesis under fluctuating light (which often happens in the field and greenhouses, e.g., Supplementary Figure 1), given that time constants of induction/relaxation of photosynthesis reduce the time-integrated rate of carbon fixation (Kromdijk et al., 2016; Morales et al., 2018). Speeding up photosynthetic induction has been suggested as an important breeding target (Tanaka et al., 2019; Qu et al., 2020). Large genotypic variation of photosynthetic induction has been found in field crops (e.g., rice, wheat, soybean, and cassava) and woody species in forestry systems, proving that breeding for improving the dynamic crop photosynthesis is feasible (Valladares et al., 1997; Soleh et al., 2017; Salter et al., 2019; Acevedo-Siaca et al., 2020; De Souza et al., 2020). Here, we show that a large genotypic variation in photosynthetic induction also exists between major horticultural crops, and generally this variation for dynamic traits is larger than the variation for steady-state traits. Also, variation between crops in photosynthetic induction was generally larger than the variation between cultivars of the same crop.

Variation of photosynthetic induction in these 19 horticultural genotypes was quantified under near-optimal conditions, i.e., climate control management in the greenhouse was done similarly as in commercial greenhouse production. This is similar to other studies that aimed to quantify genotypic variation in crops, such as rice and cassava (De Souza et al., 2020; Acevedo-Siaca et al., 2021). However, abiotic stresses often occur during crop growth, not only in the field but also in low-tech greenhouses. When testing a genotypic variation of steady-state photosynthetic traits under both well-watered and drought conditions, drought accounted for a larger proportion of total variation compared with the genotypic variation (Gu et al., 2012). Genotypic variation of dynamic photosynthetic traits could potentially be coupled with variations induced by environmental fluctuations other than irradiance. For example, genotypic variation in intrinsic water-use efficiency found in our and other studies (Acevedo-Siaca et al., 2021) could lead to different crop performance between genotypes when drought occurs. Additionally, a recent study suggested that taking into account photosynthetic induction effects led to a reduction of 2–7% in the estimation of daily carbon gain (Murakami and Jishi, 2021), which is much smaller than the estimation error predicted

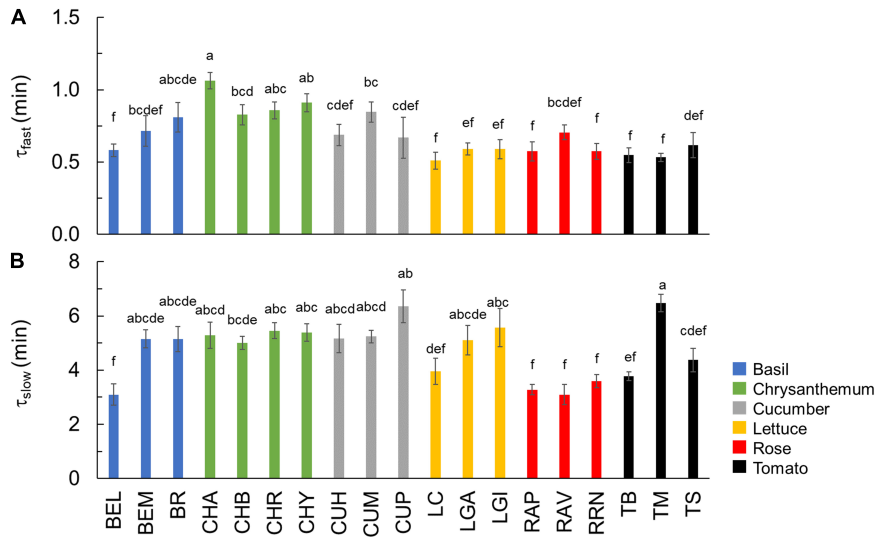


FIGURE 4 | Time constants describing the fast (**A**: τ_{fast}) and slow (**B**: τ_{slow}) phase of V_{cmax} kinetics during photosynthetic induction. Colors indicate crop species. Bars show means \pm SE ($n = 6-7$). Letters indicate significant differences ($p < 0.05$). Refer to **Table 1** for full genotype names.

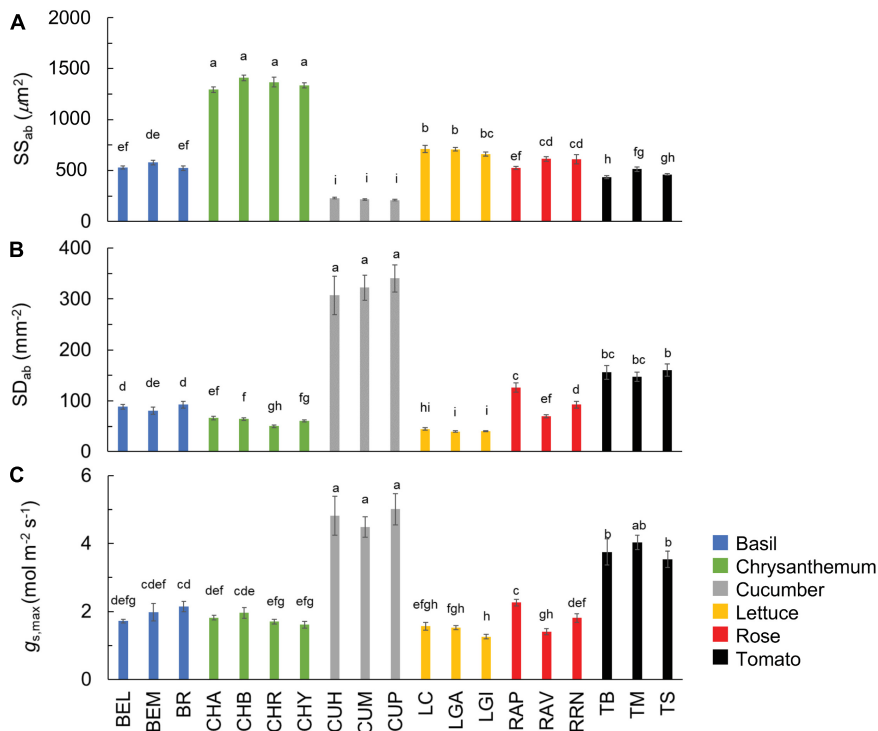
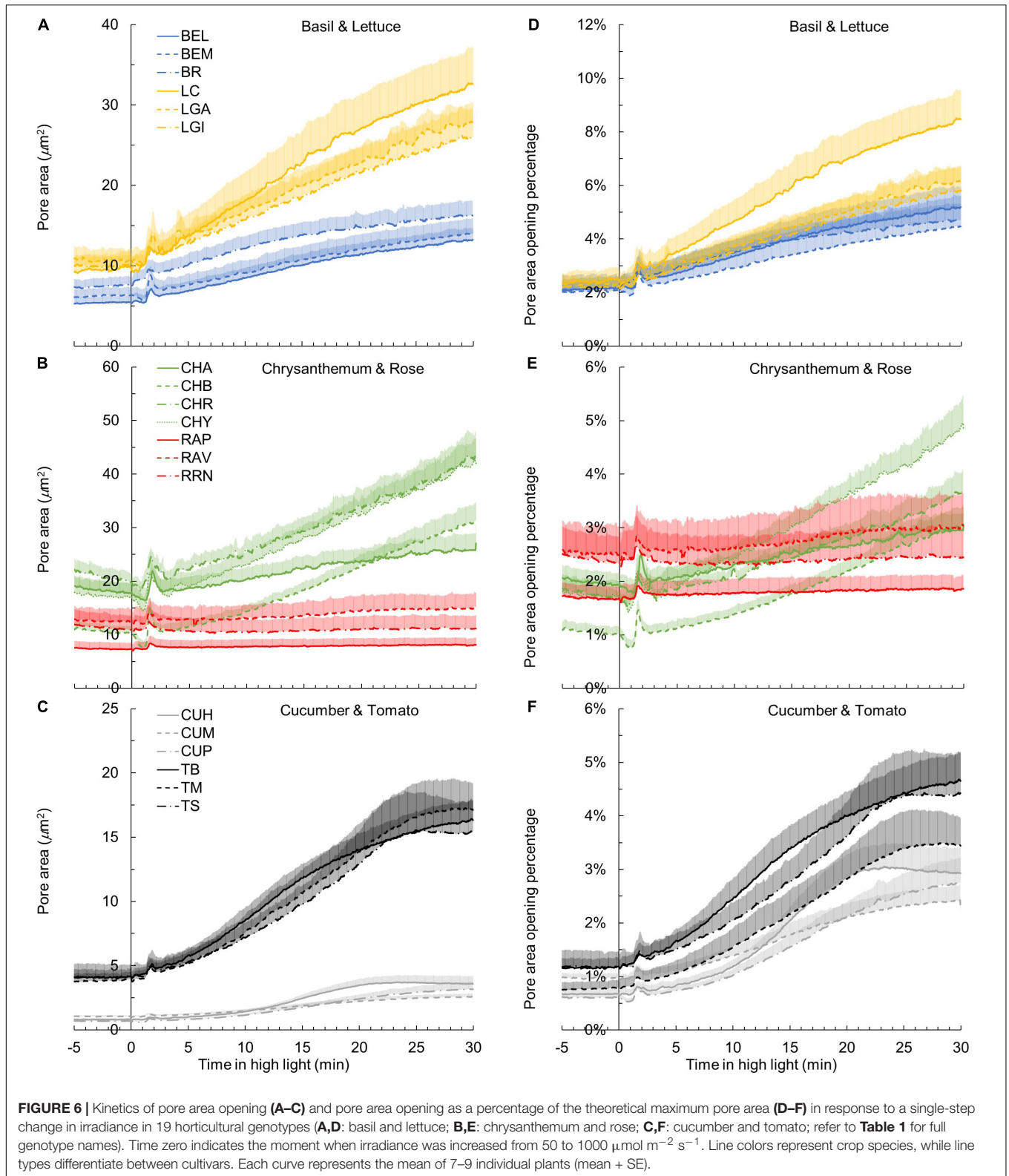


FIGURE 5 | Stomatal size (**A**; SS_{ab}) and density (**B**; SD_{ab}) at the abaxial leaf side, and theoretical maximum stomatal conductance (**C**; $g_{s,max}$) of all 19 horticultural genotypes. Colors indicate crop species. Bars show means \pm SE ($n = 7-9$). Letters indicate significant differences ($p < 0.05$). Statistical test results of SS_{ab} , SD_{ab} , and $g_{s,max}$ were based on log transformation of the data. See **Table 1** for full genotype names.

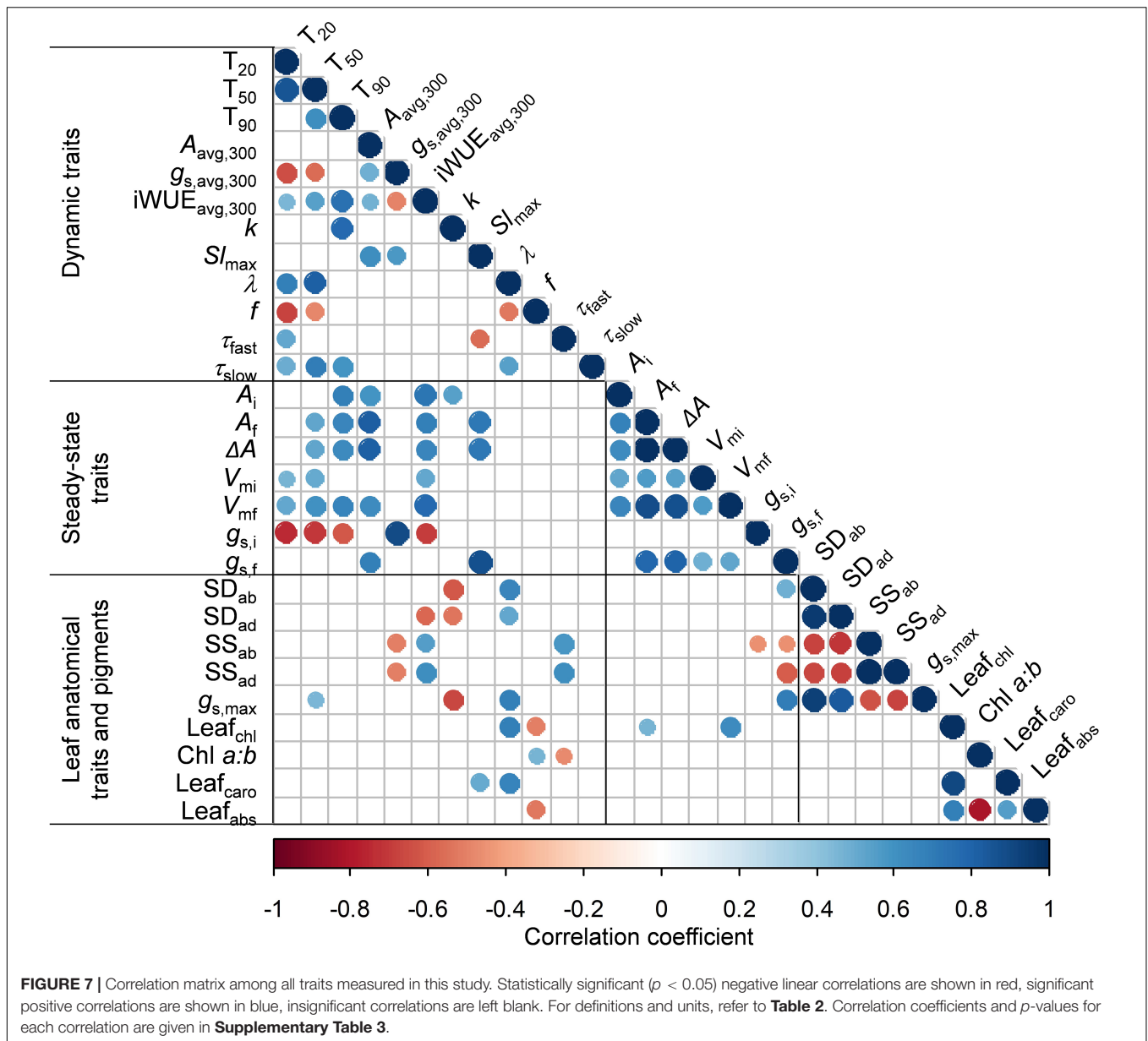
by earlier studies (Naumburg and Ellsworth, 2002; Taylor and Long, 2017) and in real measurements (Adachi et al., 2019). The patterns of irradiance fluctuations appear to be very important in determining the discrepancy between simulating daily carbon

gain with and without the effects of photosynthetic induction (Murakami and Jishi, 2021). However, only few studies quantified irradiance fluctuations in greenhouses at the relevant time scales (van Westreenen et al., 2020), hampering such estimations for the



greenhouse production context. Moreover, previous irradiances potentially affect photosynthetic induction responses to the upcoming irradiance (Jackson et al., 1991; Kaiser et al., 2017).

Further studies are needed to quantify the genotypic variation of dynamic photosynthesis under stress conditions and to evaluate their importance in different irradiance fluctuation patterns



under greenhouse conditions with considering photosynthetic induction rates across different irradiances.

Variation in Photosynthetic Induction of Horticultural Crops Is Mostly Driven by Differences in Stomatal Traits

Photosynthetic induction is mainly regulated by three transient limitations: RuBP regeneration, Rubisco activation, and stomatal opening (Percy, 1953). We found large (CV up to 68%, **Table 2**) genotypic variation in the kinetics of stomatal responses to an irradiance increase, compared to the genotypic variation in the other two limitations. A large variation in the stomatal opening time was also found across 15 vascular plants including fern, gymnosperm, and angiosperm species (Deans et al., 2019),

indicating that strong genotypic variation of stomatal response kinetics exists in many species. In our study, Sl_{max} was 0–0.3 $\mu\text{mol m}^{-2} \text{s}^{-2}$, and values for k varied between 8 and 16 min (**Table 2**). These values of Sl_{max} and k are within the range of those found for other species that had partially grown and evolved outdoors (McAusland et al., 2016), suggesting that the specific indoor growth conditions horticultural crops experienced do not influence the rapidity of stomatal opening. Faster stomatal opening tends to speed up photosynthetic induction (Shimadzu et al., 2019; Yamori et al., 2020), and our results showed a strong linear correlation between k and T_{90} (**Figure 8E**), indicating that genotypes that require less time to open their stomata reach full photosynthetic induction faster. The strong correlation between the time constants of stomatal opening and the time to approach full photosynthetic induction

also suggests that stomatal effects are typically the major ones left in the later phase of photosynthetic induction. Moreover, a higher initial g_s before an irradiance increase led to a faster speed of photosynthetic induction (**Figures 8A,C**), which is confirmatory of many previous studies (Soleh et al., 2017; Kaiser et al., 2020; Sakoda et al., 2020). These results highlight the importance of stomatal traits to explain the variations in photosynthetic induction, not only between genotypes of the same crop but also among different crops.

The speed of the stomatal response to environmental changes is generally considered to be related to the stomatal size (Hetherington and Woodward, 2003; Raven, 2014). A negative correlation exists between the stomatal size and the speed of g_s increase upon an irradiance increase, which has been found in many species (Drake et al., 2013; Kardiman and Ræbild, 2018). In addition, the relationship between average pore aperture and g_s is nonlinear (Kaiser and Kappen, 2000, 2001), which means that similar stomatal opening responses could result in different g_s kinetics, depending on the anatomical features of the stomatal complex in a given species. This nonlinear change in scale can also result in different time constants (e.g., time to reach 50% of the total variation) for the kinetic of pore aperture compared to g_s . We found that the pore area of cucumber and tomato (which had relatively small stomates) tended to reach a plateau earlier after an irradiance increase than that in chrysanthemum (which had relatively large stomates) (**Figures 5A, 6B,C**). The time needed to reach 50% of the final pore area in high irradiance was found to be higher in chrysanthemum than in cucumber and tomato (**Supplementary Figure 8**), suggesting that horticultural species with larger stomates require more time to open their stomata. However, this does not necessarily lead to a close correlation between parameters of g_s kinetics (k and $S_{l_{max}}$) and stomatal size (**Supplementary Figures 7B,C**). This could be due to the fact that stomatal density also determines g_s , and the range of genotypic variation in these traits may also be too small to identify the correlations. Both tomato and cucumber showed large absolute changes in g_s for low- and high irradiance adapted leaves (**Supplementary Figure 4**). However, changes in absolute pore area for low- and high-irradiance adapted leaves in cucumber and tomato were rather small, compared to other crops (**Figure 6C**). This could result from relatively high stomatal density in cucumber and tomato (**Figure 5B**), magnifying small changes in an individual pore area. In the hypothetical situation of a cucumber leaf having a low stomatal density, such as that of chrysanthemum, stomata in this cucumber leaf would need to open their individual pore area up to $\sim 40 \mu\text{m}^2$ to achieve the observed increase in g_s (**Supplementary Figure 9A**). In contrast, the pore area of chrysanthemum substantially increased after exposure to high irradiance, but due to a low stomatal density, this did not lead to a large increase in g_s (**Figures 5B, 6B** and **Supplementary Figure 4**). When using the hypothetical situation of a chrysanthemum leaf possessing the stomatal density of a cucumber leaf, stomata in the chrysanthemum leaf only needed to open to a very small extent ($\sim 3 \mu\text{m}^2$) to achieve the observed g_s increase (**Supplementary Figure 9B**). These results suggest that species having small but many stomates are more efficient in adjusting g_s to changes in irradiance, as it only requires

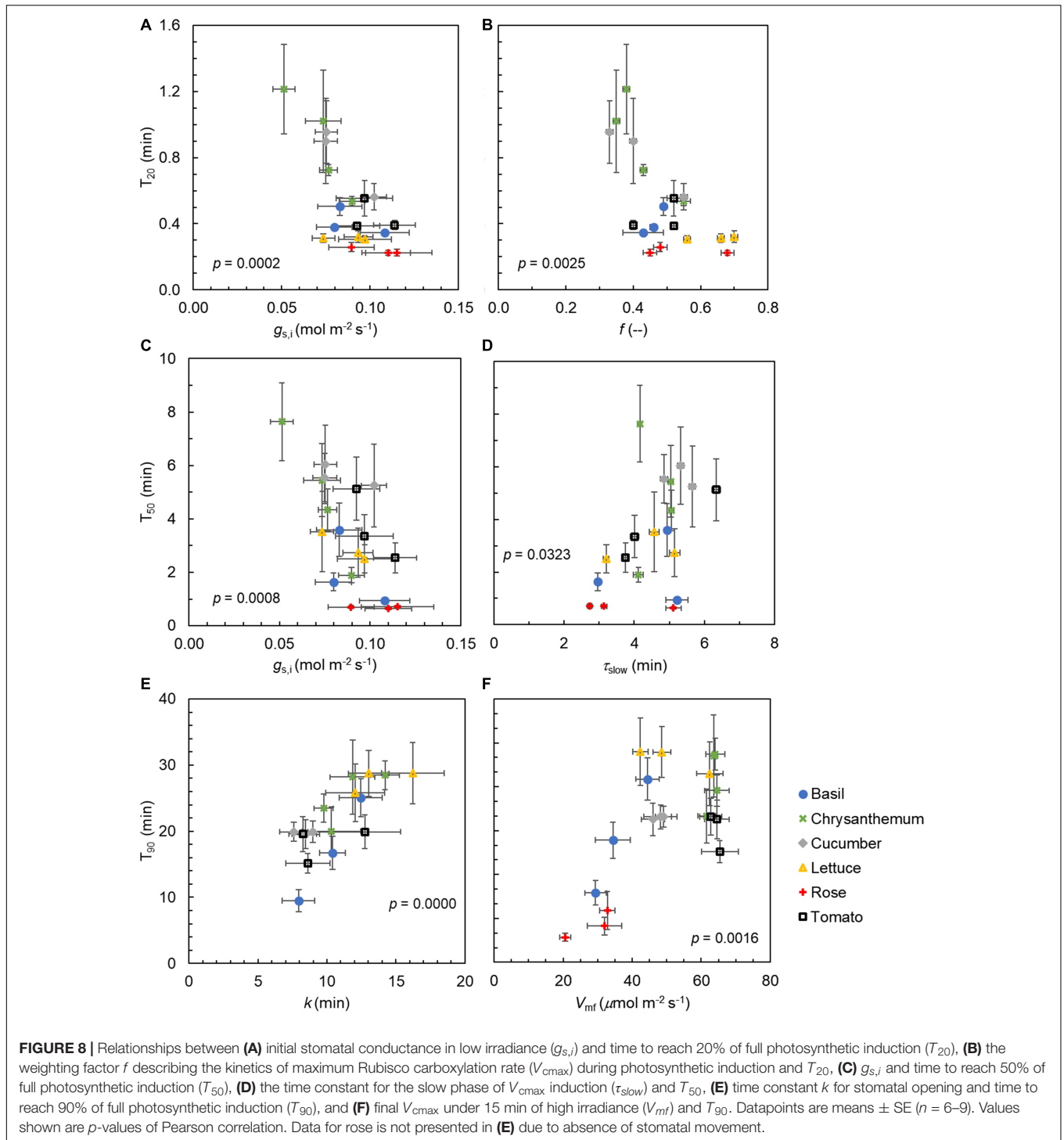
small changes in individual pores to achieve large changes in g_s .

Interestingly, the actual pore area opening generally accounted for less than 10% of the theoretical maximum pore area in all genotypes (**Figures 6D–F**), resulting in an average ratio between $g_{s,f}$ and $g_{s,max}$ (determined by anatomical traits) of 0.1 across genotypes (**Supplementary Figure 10**). This average $g_{s,f}/g_{s,max}$ ratio among horticultural crops is generally lower than what has been found in previous studies (McElwain et al., 2016; Murray et al., 2020). In a modeling study, Dow et al. (2014) predicted an optimal ratio between operating g_s and anatomical $g_{s,max}$ of 0.2; their study suggested that at 20% operating capacity, guard cells could increase the pore size efficiently when favorable conditions persisted, but could also close the pore just as quickly under stress (Dow et al., 2014). While experimental studies on the g_s - $g_{s,max}$ relationship across species are scarce, some have described a relatively constant ratio of 0.25 between operating g_s and $g_{s,max}$ in shrub and tree species (McElwain et al., 2016; Murray et al., 2020). Our results suggest that for horticultural crops, operating g_s at 10% of its maximum capacity may be already sufficient for guard cells to function efficiently.

Variation in Biochemical Processes During Photosynthetic Induction Is Less Strong Than Differences in Stomatal Traits in Horticultural Crops

The initial, fast phase of photosynthetic induction involves the availability of RuBP and other Calvin cycle intermediates and is assumed to last 1–2 min (Pearcy, 1953; Sassenrath-Cole and Pearcy, 1992). The time constant for the fast phase of $V_{c_{max}}$ induction (τ_{fast} ; **Figure 4A**) may indicate the speed of completing the initial phase of photosynthetic induction, but this assumption needs to be verified using Calvin cycle metabolomics studies. Here, τ_{fast} varied between 0.5 and 1.1 min, which is generally larger than what has been found across wheat cultivars (0.3–0.5 min; Salter et al., 2019). This may suggest higher activities and/or amounts of fructose-1,6-bisphosphatase (FBPase), sedoheptulose-1,7-bisphosphatase (SBPase), and phosphoribulokinase (PRK) in field agronomic crops than in horticultural crops, given that the activation of RuBP regeneration is mainly limited by these three enzymes (reviewed by Kaiser et al., 2018). Nevertheless, our results confirm that the time needed to complete the initial phase of photosynthetic induction is generally rapid, and this is especially true when the leaf was adapted to low irradiance instead of darkness before switching to a high irradiance (Kaiser et al., 2017), as was the case in this study.

The following, slow phase of photosynthetic induction involves light-dependent activation of Rubisco by Rubisco activase, and this phase seems to show more variation between species: time constants of 4–5 min were reported for *Alocasia macrorrhiza* and *Spinacia oleracea*, and 2–4 min for wheat (Pearcy, 1953; Salter et al., 2019). For the horticultural genotypes examined here, we found slightly larger time constants (τ_{slow}) of 3–7 min (**Figure 4B**). The rate of Rubisco activation has been found to be an important determinant of photosynthetic



induction in many species (e.g., wheat and soybean) (Soleh et al., 2017; Salter et al., 2019). However, we found a relatively smaller variation in Rubisco activation rate compared to variations found in many other traits. A CV of 22% was found for τ_{slow} , which was less than the CV of photosynthetic induction (e.g., 61% for T_{50}) and traits related to stomatal opening (e.g., 68% for Sl_{max} ; Table 2). This corresponds with the findings of

Deans et al. (2019) who found that the biochemical activation response time (5–25 min) was much more conserved between species (including angiosperms, ferns, and gymnosperms) than the time required for stomatal opening (10–150 min). It is worth noting that although the dynamic A vs. C_i approach has been used in many studies to quantify V_{cmax} kinetics during photosynthetic induction (Soleh et al., 2016; Taylor and Long, 2017; Salter et al.,

2019; De Souza et al., 2020), the original FvCB model describes steady-state photosynthesis. By applying the FvCB model on dynamic A vs. C_i , it was assumed that the slow A induction changes are mainly caused by Rubisco activation. Although the role of Rubisco activation during A induction has been verified experimentally (Taylor et al., 2022), other processes, such as changes in mesophyll conductance could also play a role during A induction (Liu et al., 2021; Sakoda et al., 2021). However, mesophyll conductance changes have been suggested to be far more rapid than the observed V_{cmax} kinetics presented here, and the relative importance of mesophyll conductance for A induction is still under debate (De Souza et al., 2020; Liu et al., 2021; Sakoda et al., 2021). We conclude that the variation in Rubisco activation kinetics among the six horticultural crops may not be the primary cause for the large variation found in photosynthetic induction.

In some species (chrysanthemum, lettuce, and tomato), photosynthetic induction in the first 1–2 min exhibited a transient drop when photosynthetic induction was measured under high CO_2 (>600 ppm; **Supplementary Figure 11**). This is likely caused by a limited amount of inorganic phosphate (Pi) in the metabolite pool of the Calvin cycle, due to insufficient and slow activation of sucrose-phosphate synthase (SPS) during the initial phase of the light increase (Stitt and Quick, 1989; Huber and Huber, 1992). Supposedly, during the first 1–2 min of the irradiance increase, the amount of free Pi is sufficient to support photosynthesis independently of any end-product synthesis. However, once Pi is exhausted, photosynthesis is inhibited until the conversion of triose-phosphates to sucrose in the cytosol releases enough Pi, which can then be translocated back into the chloroplast (Stitt and Quick, 1989). The activation of SPS is regulated by irradiance in some species (e.g., barley and maize) but not in others (e.g., soybean, tobacco, and cucumber) (Huber et al., 1989), leading to species variations in the level of Pi limitation. This may explain why in our results, the transient drop of photosynthesis in high CO_2 was seen in some species only (**Supplementary Figure 11**).

Implications for Horticultural Crop Breeding

We showed that in major horticultural crops, transient limitations to photosynthetic induction appeared to be species-dependent, but the general trend was that there was a large genotypic variation in the level of transient stomatal limitation, whereas the extent of transient non-stomatal limitation during photosynthetic induction was relatively conserved (**Supplementary Figures 5C,D**). Previous studies showed that in rice, the primary transient limitation was biochemical, whereas, in cassava, primary limitations were caused by stomata (Yamori et al., 2012; De Souza et al., 2020). For horticultural species, photosynthesis transients of some crops (e.g., cucumber) tended to be limited by biochemistry and stomata to a comparative extent, whereas those in other crops (e.g., lettuce and chrysanthemum) tended to be more strongly limited by stomata (**Supplementary Figures 5C,D**). Stomatal size may partially regulate the level of stomatal

limitation during photosynthesis induction. Species (e.g., rice) with smaller stomata have been found to show a low level of stomatal limitation (Acevedo-Siaca et al., 2020). In our study, chrysanthemum, which had the largest stomata among the tested greenhouse crops, showed the highest level of transient stomatal limitation (**Figures 3C, 5A** and **Supplementary Figure 5D**). This is possibly due to the fact that larger stomata need more time to open until a new steady state has reached (Drake et al., 2013; also refer to **Figures 6A–C** and **Supplementary Figure 8**), resulting in a higher level of transient stomatal limitation during photosynthetic induction.

Species with small stomata displayed high stomatal density, which in the case of incomplete stomatal closure may lead to high transpiration and increased water demand (e.g., during the night). Reduced stomatal density improves drought tolerance in species, such as rice and barley (Hughes et al., 2017; Caine et al., 2019). We found that the two cut-flowers have relatively low total stomatal density (including both leaf surfaces), which possibly favors vase life by increasing water conservation, such as in other cut-flowers (e.g., *Antirrhinum majus* L., Schroeder and Stimart, 2005). Altogether, these results suggest that manipulating stomatal traits rather than biochemical traits is more relevant for horticultural crop breeding.

Additionally, we found a highly conserved ratio between stomatal size at the abaxial and adaxial leaf surface, as well as between the stomatal densities on both leaf sides in all crops, except for rose (**Supplementary Figures 7E,F**). Stomatal size and density at the adaxial leaf surface were respectively 93 and 71% of the size and density at the abaxial leaf surface. A linear correlation between the stomatal densities of both leaf sides has previously been found in rice and tomato, with more stomata on the abaxial leaf surface (Fanourakis et al., 2015; Zhang et al., 2019). The distribution of stomatal density between the two leaf sides is relevant for total g_s partitioning between leaf sides (Ticha, 1982). A more uniform g_s partitioning favors CO_2 diffusion inside the leaf, and therefore gas exchange (Parkhurst and Mott, 1990; Muir et al., 2014), but may come at the expense of stress resilience in the field. Milla et al. (2013) found that wild species showed a larger difference in stomatal density between leaf sides, while domestication tended to reduce the difference of stomatal density between leaf sides, by lowering the stomatal density at the abaxial side. Interestingly, wild but not domesticated tomato genotypes showed even stomatal distribution between leaf sides (Koenig et al., 2013; Fanourakis et al., 2015). Given the potential effects of g_s partitioning between leaf sides on gas exchange, further studies are needed to explore whether or not a uniform g_s partitioning favors photosynthetic induction and the underlying mechanisms that regulate the distribution of stomatal density between leaf sides for breeding.

CONCLUSION

Large variations in the rate of photosynthetic induction were found among 19 genotypes from six of the world's most commercially relevant horticultural crops. Variations in stomatal density and size and their effects on dynamic changes in

the stomatal conductance were the major determinants of variation in the rate of photosynthetic induction, not only between crops but also between cultivars of the same crop. RuBP regeneration and Rubisco activation during photosynthetic induction exhibited relatively less genotypic variation (CV up to 22%) than did stomatal traits (CV up to 68%). Crops with large but few stomata tended to have a slow increase in stomatal conductance, potentially leading to a high level of transient stomatal limitation during photosynthetic induction. All horticultural genotypes showed an operational g_s of $\sim 10\%$ of its maximum capacity, which was lower than the average $g_s/g_{s,max}$ ratio found in previous studies. The ratio of stomatal size between abaxial and adaxial leaf surfaces was highly conserved among horticultural crops, as was the ratio of stomatal density, suggesting that the partitioning of g_s between leaf surfaces was hardly affected by species difference when under similar growth conditions. Our results highlight the importance of manipulating stomatal traits for speeding up photosynthetic induction in horticultural crops.

DATA AVAILABILITY STATEMENT

The original contributions presented in the study are included in the article/**Supplementary Material**, further inquiries can be directed to the corresponding author/s.

AUTHOR CONTRIBUTIONS

NZ, LM, and EK designed the research. NZ and SB conducted the measurements. NZ, SB, and DJ analyzed the data, with suggestions from SV-C and EK. EK and LM secured funding. NZ drafted the manuscript. SB, DJ, SV-C, LM, and EK made substantial contributions to improve the manuscript. All authors contributed to the article and approved the submitted version.

FUNDING

This project (No. 17173) was funded by the Netherlands Organisation for Scientific Research (NWO), with contributions by Signify, Glastuinbouw Nederland, Ridder Growing Solutions, and Adviesbureau JFH Snel.

ACKNOWLEDGMENTS

We thank Samikshya Shrestha and Nik Woning for analyzing stomatal images. We thank the staff of Unifarm for regular

crop management in the greenhouse, Sander van Delden for suggestions on making nutrient solutions for various greenhouse crops, Celine Nicole for help on light settings in the greenhouse, Xinyou Yin for discussion on estimating photosynthesis parameters, and Arjen vande Peppel for suggestions on measuring chlorophyll content. We thank Alejandro Morales, Jeremy Harbinson, Jan Snel, Hans Stigter, Jaap Molenaar, Ad de Koning, Dennis Medema, Celine Nicole, and Marcel Krijn for highly useful discussions. We also thank Enza Zaden, Deliflor, Nunhems/BASF, Rijk Zwaan, and Bayer Crop Science for providing seeds or plants.

SUPPLEMENTARY MATERIAL

The Supplementary Material for this article can be found online at: <https://www.frontiersin.org/articles/10.3389/fpls.2022.860229/full#supplementary-material>

Supplementary Table 1 | Ion concentrations of the nutrient solution.

Supplementary Table 2 | Stomatal pore length and guard cell width.

Supplementary Table 3 | Correlation coefficients and p -values for all focused traits (provided as a separate excel file).

Supplementary Figure 1 | Irradiance fluctuations measured in the greenhouse.

Supplementary Figure 2 | Distribution of greenhouse supplemental light.

Supplementary Figure 3 | Greenhouse climate conditions during the experiment.

Supplementary Figure 4 | Final stomatal conductance reached at low and high irradiance.

Supplementary Figure 5 | Dynamics of Rubisco carboxylation rate, electron transport rate, and transient nonstomatal and stomatal limitations during photosynthetic induction.

Supplementary Figure 6 | Leaf pigment contents and light absorbance.

Supplementary Figure 7 | Relationships between stomatal anatomical traits vs. parameters of stomatal conductance kinetics.

Supplementary Figure 8 | Time needed to reach 50% of the final pore area in high irradiance.

Supplementary Figure 9 | Kinetics of pore area opening of cucumber and chrysanthemum.

Supplementary Figure 10 | Ratio between the operating and maximum stomatal conductance.

Supplementary Figure 11 | Photosynthetic induction curves measured at different $[\text{CO}_2]$.

Supplementary Method 1 | Description of the FvCB model.

Supplementary Method 2 | Steps to solve the equation for stomatal pore area.

Supplementary Presentation 1 | Comparisons between the measured and predicted leaf net photosynthesis rates.

REFERENCES

Acevedo-Siaca, L. G., Coe, R., Quick, W. P., and Long, S. P. (2021). Variation between rice accessions in photosynthetic induction in flag leaves and underlying mechanisms. *J. Exp. Bot.* 72, 1282–1294. doi: 10.1093/jxb/eraa520

Acevedo-Siaca, L. G., Coe, R., Wang, Y., Kromdijk, J., Quick, W. P., Long, S. P., et al. (2020). Variation in photosynthetic induction between rice accessions and its potential for improving productivity. *New Phytol.* 227, 1097–1108. doi: 10.1111/nph.16454

Adachi, S., Tanaka, Y., Miyagi, A., Kashima, M., Tezuka, A., Toya, Y., et al. (2019). High-yielding rice Takanari has superior photosynthetic response to a

- commercial rice Koshihikari under fluctuating light. *J. Exp. Bot.* 70, 5287–5297. doi: 10.1093/jxb/erz304
- Allen, M. T., and Percy, R. W. (2000). Stomatal versus biochemical limitations to dynamic photosynthetic performance in four tropical rainforest shrub species. *Oecologia* 122, 479–486. doi: 10.1007/s004420050969
- Caine, R. S., Yin, X., Sloan, J., Harrison, E. L., Mohammed, U., Fulton, T., et al. (2019). Rice with reduced stomatal density conserves water and has improved drought tolerance under future climate conditions. *New Phytol.* 221, 371–384. doi: 10.1111/nph.15344
- Carvalho, S. M. P., and Heuvelink, E. (2003). Effect of assimilate availability on flower characteristics and plant height of cut *Chrysanthemum*: an integrated study. *J. Hortic. Sci. Biotechnol.* 78, 711–720. doi: 10.1080/14620316.2003.11511688
- De Souza, A. P., Wang, Y., Orr, D. J., Carmo-Silva, E., and Long, S. P. (2020). Photosynthesis across African cassava germplasm is limited by Rubisco and mesophyll conductance at steady state, but by stomatal conductance in fluctuating light. *New Phytol.* 225, 2498–2512. doi: 10.1111/nph.16142
- Deans, R. M., Brodribb, T. J., Busch, F. A., and Farquhar, G. D. (2019). Plant water-use strategy mediates stomatal effects on the light induction of photosynthesis. *New Phytol.* 222, 382–395. doi: 10.1111/nph.15572
- Dow, G. J., Bergmann, D. C., and Berry, J. A. (2014). An integrated model of stomatal development and leaf physiology. *New Phytol.* 201, 1218–1226. doi: 10.1111/nph.12608
- Drake, P. L., Froend, R. H., and Franks, P. J. (2013). Smaller, faster stomata: scaling of stomatal size, rate of response, and stomatal conductance. *J. Exp. Bot.* 64, 495–505. doi: 10.1093/jxb/ers347
- Elliott-Kingston, C., Haworth, M., Yearsley, J. M., Batke, S. P., Lawson, T., and McElwain, J. C. (2016). Does size matter? Atmospheric CO₂ may be a stronger driver of stomatal closing rate than stomatal size in taxa that diversified under low CO₂. *Front. Plant Sci.* 7:1253. doi: 10.3389/fpls.2016.01253
- Fanourakis, D., Giday, H., Milla, R., Pieruschka, R., Kjaer, K. H., Bolger, M., et al. (2015). Pore size regulates operating stomatal conductance, while stomatal densities drive the partitioning of conductance between leaf sides. *Ann. Bot.* 115, 555–565. doi: 10.1093/aob/mcu247
- Farquhar, G. D., von Caemmerer, S., and Berry, J. A. (1980). A biochemical model of photosynthetic CO₂ assimilation in leaves of C₃ species. *Planta* 149, 78–90. doi: 10.1007/BF00386231
- Flood, P. J., Harbinson, J., and Aarts, M. G. M. (2011). Natural genetic variation in plant photosynthesis. *Trends Plant Sci.* 16, 327–335. doi: 10.1016/j.tplants.2011.02.005
- Franks, P. J., and Beerling, D. J. (2009). Maximum leaf conductance driven by CO₂ effects on stomatal size and density over geologic time. *Proc. Natl. Acad. Sci. U.S.A.* 106, 10343–10347. doi: 10.1073/pnas.0904209106
- Franks, P. J., and Farquhar, G. D. (2001). The effect of exogenous abscisic acid on stomatal development, stomatal mechanics, and leaf gas exchange in *Tradescantia virginiana*. *Plant Physiol.* 125, 935–942. doi: 10.1104/pp.125.2.935
- Giday, H., Kjaer, K. H., Fanourakis, D., and Ottosen, C. O. (2013). Smaller stomata require less severe leaf drying to close: a case study in *Rosa hybrida*. *J. Plant Physiol.* 170, 1309–1316. doi: 10.1016/j.jplph.2013.04.007
- Gu, J., Yin, X., Stomph, T.-J., Wang, H., and Struik, P. C. (2012). Physiological basis of genetic variation in leaf photosynthesis methylation and chromatin patterning among rice (*Oryza sativa* L.) introgression lines under drought and well-watered conditions. *J. Exp. Bot.* 63, 5137–5153. doi: 10.1093/jxb/ers170
- Hetherington, A. M., and Woodward, F. I. (2003). The role of stomata in sensing and driving environmental change. *Nature* 424, 901–908. doi: 10.4135/9781446201091.n40
- Hogewoning, S. W., Douwstra, P., Trouwborst, G., Van Ieperen, W., and Harbinson, J. (2010). An artificial solar spectrum substantially alters plant development compared with usual climate room irradiance spectra. *J. Exp. Bot.* 61, 1267–1276. doi: 10.1093/jxb/erq005
- Huber, S. C., and Huber, J. L. (1992). Role of sucrose-phosphate synthase in sucrose metabolism in leaves. *Plant Physiol.* 99, 1275–1278. doi: 10.1104/pp.99.4.1275
- Huber, S. C., Nielsen, T. H., Huber, J. L. A., and Pharr, D. M. (1989). Variation among species in light activation of sucrose-phosphate synthase. *Plant Cell Physiol.* 30, 277–285. doi: 10.1104/pp.108.4.1665
- Hughes, J., Hepworth, C., Dutton, C., Dunn, J. A., Hunt, L., Stephens, J., et al. (2017). Reducing stomatal density in barley improves drought tolerance without impacting on yield. *Plant Physiol.* 174, 776–787. doi: 10.1104/pp.16.01844
- Jackson, R. B., Woodrow, I. E., and Mott, K. A. (1991). Nonsteady-state photosynthesis following an increase in photon flux density (PFD): effects of magnitude and duration of initial PFD. *Plant Physiol.* 95, 498–503. doi: 10.1104/pp.95.2.498
- Kaiser, E., Morales, A., and Harbinson, J. (2018). Fluctuating light takes crop photosynthesis on a rollercoaster ride. *Plant Physiol.* 176, 977–989. doi: 10.1104/pp.17.01250
- Kaiser, E., Morales, A., Harbinson, J., Heuvelink, E., and Marcelis, L. F. M. (2020). High stomatal conductance in the tomato flacca mutant allows for faster photosynthetic induction. *Front. Plant Sci.* 11:1317. doi: 10.3389/fpls.2020.01317
- Kaiser, E., Morales, A., Harbinson, J., Heuvelink, E., Prinzenberg, A. E., and Marcelis, L. F. M. (2016). Metabolic and diffusional limitations of photosynthesis in fluctuating irradiance in *Arabidopsis thaliana*. *Sci. Rep.* 6:31252. doi: 10.1038/srep31252
- Kaiser, E., Morales, A., Harbinson, J., Kromdijk, J., Heuvelink, E., and Marcelis, L. F. M. (2015). Dynamic photosynthesis in different environmental conditions. *J. Exp. Bot.* 66, 2415–2426. doi: 10.1093/jxb/eru406
- Kaiser, E., Zhou, D., Heuvelink, E., Harbinson, J., Morales, A., and Marcelis, L. F. M. (2017). Elevated CO₂ increases photosynthesis in fluctuating irradiance regardless of photosynthetic induction state. *J. Exp. Bot.* 68, 5629–5640. doi: 10.1093/jxb/erx357
- Kaiser, H., and Kappen, L. (2000). In situ observation of stomatal movements and gas exchange of *Aegopodium podagraria* L. in the understorey. *J. Exp. Bot.* 51, 1741–1749. doi: 10.1093/jexbot/51.351.1741
- Kaiser, H., and Kappen, L. (2001). Stomatal oscillations at small apertures: indications for a fundamental insufficiency of stomatal feedback-control inherent in the stomatal turgor mechanism. *J. Exp. Bot.* 52, 1303–1313. doi: 10.1093/jxb/52.359.1303
- Kardiman, R., and Røebild, A. (2018). Relationship between stomatal density, size and speed of opening in Sumatran rainforest species. *Tree Physiol.* 38, 696–705. doi: 10.1093/treephys/tpx149
- Koenig, D., Jiménez-Gómez, J. M., Kimura, S., Fulop, D., Chitwood, D. H., Headland, L. R., et al. (2013). Comparative transcriptomics reveals patterns of selection in domesticated and wild tomato. *Proc. Natl. Acad. Sci. U.S.A.* 110, 2–9. doi: 10.1073/pnas.1309606110
- Kromdijk, J., Glowacka, K., Leonelli, L., Gabilly, S. T., Iwai, M., Niyogi, K. K., et al. (2016). Improving photosynthesis and crop productivity by accelerating recovery from photoprotection. *Science* 354, 857–862. doi: 10.1126/science.aai8878
- Laisk, A. K. (1977). *Kinetics of Photosynthesis and Photorespiration of C₃ in Plants* (in Russian). Moscow: Nauk.
- Lawson, T., and Viallet-Chabrand, S. (2019). Speedy stomata, photosynthesis and plant water use efficiency. *New Phytol.* 221, 93–98. doi: 10.1111/nph.15330
- Li, T., Heuvelink, E., and Marcelis, L. F. M. (2015). Quantifying the source-sink balance and carbohydrate content in three tomato cultivars. *Front. Plant Sci.* 6:416. doi: 10.3389/fpls.2015.00416
- Liu, T., Barbour, M. M., Yu, D., Rao, S., and Song, X. (2021). Mesophyll conductance exerts a significant limitation on photosynthesis during light induction. *New Phytol.* 233, 360–372. doi: 10.1111/nph.17757
- Marcelis, L. F. M. (1994). A simulation model for dry matter partitioning in cucumber. *Ann. Bot.* 74, 43–52. doi: 10.1093/aob/74.1.43
- Marcelis, L. F. M., Kaiser, E., Van Westreenen, A., and Heuvelink, E. (2018). Sustainable crop production in greenhouses based on understanding crop physiology. *Acta Hortic.* 1227, 1–12. doi: 10.17660/ActaHortic.2018.1227.1
- McAusland, L., Viallet-Chabrand, S., Davey, P., Baker, N. R., Brendel, O., and Lawson, T. (2016). Effects of kinetics of light-induced stomatal responses on photosynthesis and water-use efficiency. *New Phytol.* 211, 1209–1220. doi: 10.1111/nph.14000
- McAusland, L., Viallet-Chabrand, S., Jauregui, I., Burridge, A., Hubbert-Edwards, S., Fryer, M. J., et al. (2020). Variation in key leaf photosynthetic traits across wheat wild relatives is accession dependent not species dependent. *New Phytol.* 228, 1767–1780. doi: 10.1111/nph.16832
- McElwain, J. C., Yirotis, C., and Lawson, T. (2016). Using modern plant trait relationships between observed and theoretical maximum stomatal

- conductance and vein density to examine patterns of plant macroevolution. *New Phytol.* 209, 94–103. doi: 10.1111/nph.13579
- Milla, R., De Diego-Vico, N., and Martín-Robles, N. (2013). Shifts in stomatal traits following the domestication of plant species. *J. Exp. Bot.* 64, 3137–3146. doi: 10.1093/jxb/ert147
- Morales, A., Kaiser, E., Yin, X., Harbinson, J., Molenaar, J., Driever, S. M., et al. (2018). Dynamic modelling of limitations on improving leaf CO₂ assimilation under fluctuating irradiance. *Plant Cell Environ.* 41, 589–604. doi: 10.1111/pce.13119
- Mott, K. A., and Woodrow, I. E. (2000). Modelling the role of Rubisco activase in limiting non-steady-state photosynthesis. *J. Exp. Bot.* 51, 399–406. doi: 10.1093/jxb/51.suppl_1.399
- Muir, C. D., Hangarter, R. P., Moyle, L. C., and Davis, P. A. (2014). Morphological and anatomical determinants of mesophyll conductance in wild relatives of tomato (*Solanum* sect. *Lycopersicon*, sect. *Lycopersicoideae*; Solanaceae). *Plant Cell Environ.* 37, 1415–1426. doi: 10.1111/pce.12245
- Murakami, K., and Jishi, T. (2021). Appropriate time interval of PPFD measurement to estimate daily photosynthetic gain. *Funct. Plant Biol.* [Epub ahead of print]. doi: 10.1071/FP20323
- Murray, M., Soh, W. K., Yiotis, C., Spicer, R. A., Lawson, T., and McElwain, J. C. (2020). Consistent relationship between field-measured stomatal conductance and theoretical maximum stomatal conductance in C₃ woody angiosperms in four major biomes. *Int. J. Plant Sci.* 181, 142–154. doi: 10.1086/706260
- Naumburg, E., and Ellsworth, D. S. (2002). Short-term light and leaf photosynthetic dynamics affect estimates of daily understory photosynthesis in four tree species. *Tree Physiol.* 22, 393–401. doi: 10.1093/treephys/22.6.393
- Ort, D. R., Merchant, S. S., Alric, J., Barkan, A., Blankenship, R. E., Bock, R., et al. (2015). Redesigning photosynthesis to sustainably meet global food and bioenergy demand. *Proc. Natl. Acad. Sci. U.S.A.* 112, 8529–8536.
- Parkhurst, D. F., and Mott, K. A. (1990). Intercellular diffusion limits to CO₂ uptake in leaves: studies in air and helox. *Plant Physiol.* 94, 1024–1032. doi: 10.1104/pp.94.3.1024
- Pearcy, R. W. (1953). Photosynthesis in plant life. *J. Franklin Inst.* 256, 599–600. doi: 10.1016/0016-0032(53)91189-2
- Qu, M., Essemine, J., Xu, J., Ablat, G., Perveen, S., Wang, H., et al. (2020). Alterations in stomatal response to fluctuating light increase biomass and yield of rice under drought conditions. *Plant J.* 104, 1334–1347.
- Raven, J. A. (2014). Speedy small stomata? *J. Exp. Bot.* 65, 1415–1424. doi: 10.1093/jxb/eru032
- Sakoda, K., Yamori, W., Groszmann, M., and Evans, J. R. (2021). Stomatal, mesophyll conductance, and biochemical limitations to photosynthesis during induction. *Plant Physiol.* 185, 146–160. doi: 10.1093/plphys/kiaa011
- Sakoda, K., Yamori, W., Shimada, T., Sugano, S. S., Hara-Nishimura, I., and Tanaka, Y. (2020). Higher stomatal density improves photosynthetic induction and biomass production in *Arabidopsis* under fluctuating light. *Front. Plant Sci.* 11:589603. doi: 10.3389/fpls.2020.589603
- Salter, W. T., Merchant, A. M., Richards, R. A., Trethowan, R., and Buckley, T. N. (2019). Rate of photosynthetic induction in fluctuating light varies widely among genotypes of wheat. *J. Exp. Bot.* 70, 2787–2796. doi: 10.1093/jxb/erz100
- Sassenrath-Cole, G. F., and Pearcy, R. W. (1992). The role of ribulose-1,5-bisphosphate regeneration in the induction requirement of photosynthetic CO₂ exchange under transient light conditions. *Plant Physiol.* 99, 227–234. doi: 10.1104/pp.99.1.227
- Schroeder, K. R., and Stimart, D. P. (2005). Comparison of stomatal density and postharvest transpiration between long- and short-lived cut flower genotypes of *Antirrhinum majus* L. *J. Am. Soc. Hortic. Sci.* 130, 742–746. doi: 10.21273/jashs.130.5.742
- Shimadzu, S., Seo, M., Terashima, I., and Yamori, W. (2019). Whole irradiated plant leaves showed faster photosynthetic induction than individually irradiated leaves via improved stomatal opening. *Front. Plant Sci.* 10:1512. doi: 10.3389/fpls.2019.01512
- Simkin, A. J., López-Calcagno, P. E., and Raines, C. A. (2019). Feeding the world: improving photosynthetic efficiency for sustainable crop production. *J. Exp. Bot.* 70, 1119–1140. doi: 10.1093/jxb/ery445
- Slattery, R. A., Walker, B. J., Weber, A. P. M., and Ort, D. R. (2018). The impacts of fluctuating light on crop performance. *Plant Physiol.* 176, 990–1003. doi: 10.1104/pp.17.01234
- Soleh, M. A., Tanaka, Y., Kim, S. Y., Huber, S. C., Sakoda, K., and Shiraiwa, T. (2017). Identification of large variation in the photosynthetic induction response among 37 soybean [*Glycine max* (L.) Merr.] genotypes that is not correlated with steady-state photosynthetic capacity. *Photosynth. Res.* 131, 305–315. doi: 10.1007/s11120-016-0323-1
- Soleh, M. A., Tanaka, Y., Nomoto, Y., Iwahashi, Y., Nakashima, K., Fukuda, Y., et al. (2016). Factors underlying genotypic differences in the induction of photosynthesis in soybean [*Glycine max* (L.) Merr.]. *Plant Cell Environ.* 39, 685–693.
- Stitt, M., and Quick, W. P. (1989). Photosynthetic carbon partitioning: its regulation and possibilities for manipulation. *Physiol. Plant.* 77, 633–641.
- Tanaka, Y., Adachi, S., and Yamori, W. (2019). Natural genetic variation of the photosynthetic induction response to fluctuating light environment. *Curr. Opin. Plant Biol.* 49, 52–59. doi: 10.1016/j.pbi.2019.04.010
- Taylor, S. H., Gonzalez-Escobar, E., Page, R., Parry, M. A., Long, S. P., and Carmo-Silva, E. (2022). Faster than expected Rubisco deactivation in shade reduces cowpea photosynthetic potential in variable light conditions. *Nat. Plants* 8, 118–124. doi: 10.1038/s41477-021-01068-9
- Taylor, S. H., and Long, S. P. (2017). Slow induction of photosynthesis on shade to sun transitions in wheat may cost at least 21% of productivity. *Philos. Trans. R. Soc. B Biol. Sci.* 372:20160543. doi: 10.1098/rstb.2016.0543
- Ticha, I. (1982). Photosynthetic characteristics during ontogenesis of leaves. VII. stomata density and sizes. *Photosynthetica* 16, 375–471.
- Valladares, F., Allen, M. T., and Pearcy, R. W. (1997). Photosynthetic responses to dynamic light under field conditions in six tropical rainforest shrubs occurring along a light gradient. *Oecologia* 111, 505–514. doi: 10.1007/s004420050264
- van Westreenen, A., Zhang, N., Douma, J. C., Evers, J. B., Anten, N. P. R., and Marcelis, L. F. M. (2020). Substantial differences occur between canopy and ambient climate: quantification of interactions in a greenhouse-canopy system. *PLoS One* 15:e0233210. doi: 10.1371/journal.pone.0233210
- Violet-Chabrand, S., Dreyer, E., and Brendel, O. (2013). Performance of a new dynamic model for predicting diurnal time courses of stomatal conductance at the leaf level. *Plant Cell Environ.* 36, 1529–1546. doi: 10.1111/pce.12086
- Wang, Y. P., and Jarvis, P. G. (1993). Influence of shoot structure on the photosynthesis of Sitka spruce (*Picea sitchensis*). *Funct. Ecol.* 7, 433–451.
- Wellburn, A. R. (1994). The spectral determination of chlorophylls a and b, as well as total carotenoids, using various solvents with spectrophotometers of different resolution. *J. Plant Physiol.* 144, 307–313. doi: 10.1016/S0176-1617(11)81192-2
- Yamori, W., Kusumi, K., Iba, K., and Terashima, I. (2020). Increased stomatal conductance induces rapid changes to photosynthetic rate in response to naturally fluctuating light conditions in rice. *Plant Cell Environ.* 43, 1230–1240. doi: 10.1111/pce.13725
- Yamori, W., Masumoto, C., Fukayama, H., and Makino, A. (2012). Rubisco activase is a key regulator of non-steady-state photosynthesis at any leaf temperature and, to a lesser extent, of steady-state photosynthesis at high temperature. *Plant J.* 71, 871–880. doi: 10.1111/j.1365-313X.2012.05041.x
- Zhang, N., Van Westreenen, A., Evers, J. B., Anten, N. P. R., and Marcelis, L. F. M. (2020). Quantifying the contribution of bent shoots to plant photosynthesis and biomass production of flower shoots in rose (*Rosa hybrida*) using a functional-structural plant model. *Ann. Bot.* 126, 587–599. doi: 10.1093/aob/mcz150
- Zhang, Q., Peng, S., and Li, Y. (2019). Increase rate of light-induced stomatal conductance is related to stomatal size in the genus *Oryza*. *J. Exp. Bot.* 70, 5259–5269.

Conflict of Interest: The authors declare that the research was conducted in the absence of any commercial or financial relationships that could be construed as a potential conflict of interest.

Publisher's Note: All claims expressed in this article are solely those of the authors and do not necessarily represent those of their affiliated organizations, or those of the publisher, the editors and the reviewers. Any product that may be evaluated in this article, or claim that may be made by its manufacturer, is not guaranteed or endorsed by the publisher.

Copyright © 2022 Zhang, Berman, Joubert, Violet-Chabrand, Marcelis and Kaiser. This is an open-access article distributed under the terms of the Creative Commons Attribution License (CC BY). The use, distribution or reproduction in other forums is permitted, provided the original author(s) and the copyright owner(s) are credited and that the original publication in this journal is cited, in accordance with accepted academic practice. No use, distribution or reproduction is permitted which does not comply with these terms.